NAVAL POSTGRADUATE SCHOOL
MONTEREY, CALIFORNIA

THESIS

THERMOMECHANICAL PROCESSING OF AN AL ALLOY 2519, AND AN ASSESSMENT OF ITS SUPERPLASTIC RESPONSE

by

Benjamin Braman Peet

March, 1995

Thesis Advisor: Terry R. McNelley

Approved for public release; distribution is unlimited.

REPORT DOCUMENTATION PAGE

Form Approved OMB No. 0704-0188

1. AGENCY USE ONLY *(Leave blank)*	2. REPORT DATE March 1995	3. REPORT TYPE AND DATES COVERED Master's Thesis

4. THERMOMECHANICAL PROCESSING OF AN AL ALLOY 2519, AND AN ASSESSMENT OF ITS SUPERPLASTIC RESPONSE

5. FUNDING NUMBERS

6. AUTHOR(S) Peet, Benjamin B.

7. PERFORMING ORGANIZATION NAME(S) AND ADDRESS(ES)
Naval Postgraduate School
Monterey CA 93943-5000

8. PERFORMING ORGANIZATION REPORT NUMBER

9. SPONSORING/MONITORING AGENCY NAME(S) AND ADDRESS(ES)

10. SPONSORING/MONITORING AGENCY REPORT NUMBER

11. SUPPLEMENTARY NOTES The views expressed in this thesis are those of the author and do not reflect the official policy or position of the Department of Defense or the U.S. Government.

12a. DISTRIBUTION/AVAILABILITY STATEMENT
Approved for public release; distribution is unlimited.

12b. DISTRIBUTION CODE

13. ABSTRACT *(maximum 200 words)*

The effects of different overaging temperatures and times prior to the rolling portion of a thermomechanical process (TMP) were examined to determine those combinations resulting in refined microstructures capable of supporting superplastic behavior. Specimens of processed Al 2519 were tension tested at elevated temperatures after varying TMP parameters. Enhanced ductility in comparison to unprocessed material was observed at all test temperatures in the range of 300-450°C. Moderate superplastic ductilities (up to 300%) were encountered under some conditions. Backscattered electron imaging techniques coupled with quantitative microstructural analysis methods were used to examine both processed and deformed samples. The correlations among processing, microstructure and mechanical behavior are presented.

14. SUBJECT TERMS Superplastic deformation of aluminum alloy 2519

15. NUMBER OF PAGES 62

16. PRICE CODE

17. SECURITY CLASSIFICATION OF REPORT	18. SECURITY CLASSIFICATION OF THIS PAGE	19. SECURITY CLASSIFICATION OF ABSTRACT	20. LIMITATION OF ABSTRACT
Unclassified	Unclassified	Unclassified	UL

NSN 7540-01-280-5500 Standard Form 298 (Rev. 2-89)
Prescribed by ANSI Std. 239-18 298-102

Approved for public release; distribution is unlimited.

THERMOMECHANICAL PROCESSING OF AN AL ALLOY 2519, AND AN ASSESSMENT OF ITS SUPERPLASTIC RESPONSE

by

Benjamin B. Peet
Lieutenant, United States Navy
B.S., United States Naval Academy, 1988

Submitted in partial fulfillment
of the requirements for the degree of

MASTER OF SCIENCE IN MECHANICAL ENGINEERING

from the

NAVAL POSTGRADUATE SCHOOL
March 1995

Author: Benjamin B Peet
Benjamin B. Peet

Approved by: T R McNelley
Terry R. McNelley, Thesis Advisor

Matthew Kelleher
Matthew D. Kelleher, Chairman
Department of Mechanical Engineering

ABSTRACT

The effects of different overaging temperatures and times prior to the rolling portion of a thermomechanical process (TMP) were examined to determine those combinations resulting in refined microstructures capable of supporting superplastic behavior. Specimens of processed Al 2519 were tension tested at elevated temperatures after varying TMP parameters. Enhanced ductility in comparison to unprocessed material was observed at all test temperatures in the range of 300-450°C. Moderate superplastic ductilities (up to 300%) were encountered under some conditions. Backscattered electron imaging techniques coupled with quantitative microstructural analysis methods were used to examine both processed and deformed samples. The correlations among processing, microstructure and mechanical behavior are presented.

TABLE OF CONTENTS

I. INTRODUCTION

Superplastic materials are characterized by the ability to deform plastically without localized necking. Elongations above 200 percent can be termed moderately superplastic while 1000 percent or more is a highly superplastic response. Two types of superplasticity are currently recognized, isothermal and transformation. Isothermal superplasticity is of current interest for commercial development due to its similarity to processes used in conventional metal forming. Existing techniques include the Supral and Rockwell methods which use Al-Cu-Zr and Al-Zn-Mg-Cu alloys, respectively. The Supral process utilizes additions of zirconium to form fine AL_3Zr particles that impede grain growth [Ref. 1]. Continuous recrystallization is promoted during deformation, resulting in refinement of the grain size; superplastic deformation is typically accomplished at 460°C. The Rockwell method employs overaging and cold working to refine the grain structure of the material. Second-phase particles are precipitated during overaging and provide nucleation sites for new grains upon a recrystallization treatment. [Ref. 2] These materials and processes are more expensive than conventional aluminum processing.

Present applications of superplastically formed materials include light-weight radar dishes and coolant piping for fire control radars [Ref. 3], B-1B landing gear doors [Ref. 4] and many structures fabricated for the F/A-18A Hornet aircraft from either aluminum or titanium alloys [Ref. 5]. The enhanced ductility of superplastic materials allows the forming of intricate shapes from a single piece. Since fewer parts are required to form complex assemblies, the number of fasteners can be reduced this in turn has many benefits; stress concentrations which can lead to fatigue may be eliminated and resistance to corrosion can be enhanced, weight savings can be realized, dimensional accuracy is better, and assembly time and maintenance are reduced as well. A typical example is the girder assembly in the lower avionics deck of the F-5E jet aircraft. Superplastic forming of this structural member allowed the piece to be made using eight tools, five parts and less than

12 manhours of labor; this is 126 tools and 43 parts less than conventional techniques at a savings of 33 manhours [Ref. 6].

A substantial amount of work on Al-Mg alloys has been done at the Naval Post graduate school. By adjusting the thermomechanical processing (TMP) schedules used on this alloy, elongations in excess of 1000 percent were achieved at test temperatures of 300°C and strain rates of approximately 10^{-3} sec^{-1} [Ref. 7]. This superplastic deformation has been theorized to be the result of particle stimulated nucleation (PSN) during TMP, which provides refinement of the initial grain structure by recrystallization at sites supplied by sufficiently large precipitates.

The possibility of similar microstructural refinement in an Al-Cu alloy has been examined in a series of four previous efforts. Mathé examined the microstructures produced during prolonged annealing; overaging times ranged up to 500 hours and temperatures up to 500°C. Maximum elongation of ~205 percent was attained in material overaged at 350°C, subsequently rolled at 350°C and tested at 450°C [Ref. 8]. Bohman overaged at 450°C only and tested at temperatures from 300 to 400°C. His maximum elongation was 260 percent for a specimen tested at 450°C [Ref. 9]. Dunlap attempted to determine the critical radius of the θ (Al_2Cu) particles required to stimulate nucleation. He performed numerous TMP's and developed a method to estimate the critical size for each TMP. His grain size was refined to a 10-12 μm average diameter [Ref. 10]. Zohorsky attempted to gain more control over the size and distribution of the second phase particles and devised numerous new TMP's to do this. He found that rolling done at room temperature was best able to provide the prestrain required to reduce the aluminum grain size a sufficient amount to support superplastic response. He produced numerous materials to be tested and surmised that a sample overaged at 200°C for 50 hours and then 400°C for 50 hours would have the most refined grain structure and hence the greatest superplastic response [Ref. 11].

The objective of this thesis is first, to devise a test protocol with new apparatus that would allow testing of samples at constant engineering strain rates and elevated temperatures with a variation in test temperature over the entire test section not to exceed one degree Celsius. Second, testing of all promising material from earlier work by Zohorsky was to be done and microstructural analysis produced to determine the average grain diameter, θ particle size and volume fraction. Finally additional processing was to be accomplished in order to further investigate trends in superplastic response related to process history.

II. BACKGROUND

A. ALUMINUM ALLOYS

The alloy Al 2519 was chosen for this study based on it's high copper content which allows a large volume percent of the θ phase to be formed. For a given particle size, a higher volume fraction will result in a smaller particle spacing; this is important in the (PSN) theory covered in the next section.

Aluminum alloys offer many benefits especially if weight is of critical importance. Various alloys can be cast, wrought, welded and machined; many also offer good corrosion resistance. The high strength-to-weight ratio of aluminum can be useful in aircraft applications were significant fuel savings can be realized [Ref. 12]. The alloy used in this study, Al 2519, is a wrought alloy with 6.06 wt. pct. Cu; this high percentage of Cu allows good weldability because of back-filling by eutectic liquid in the weld pool and hence reduced susceptibility to weld cracking [Ref. 13]. Figure 2.1 shows the binary aluminum copper phase diagram [Ref. 14].

In order to increase the strength of a metal such as aluminum, dislocation motion must be retarded [Ref. 15]. Three major ways to achieve this are strain hardening, solid solution strengthening and precipitation hardening. Strain hardening uses plastic deformation of the material to create a certain dislocation density. The interaction of these dislocations inhibits the free movement of other dislocations [Ref. 6]. Solid solution strengthening relies on the ability of aluminum to dissolve other elements. Solute atoms may substitute for the aluminum atoms in the crystal structure and, if different in size, they produce a strain field. The greater the size difference the greater the induced stress but the lower the solubility. The strain field of the solute interacts with dislocation stress fields, inhibiting dislocation rotation and thereby strengthening the material. As the limit of solubility is exceeded dispersion, or precipitation, strengthening takes hold.

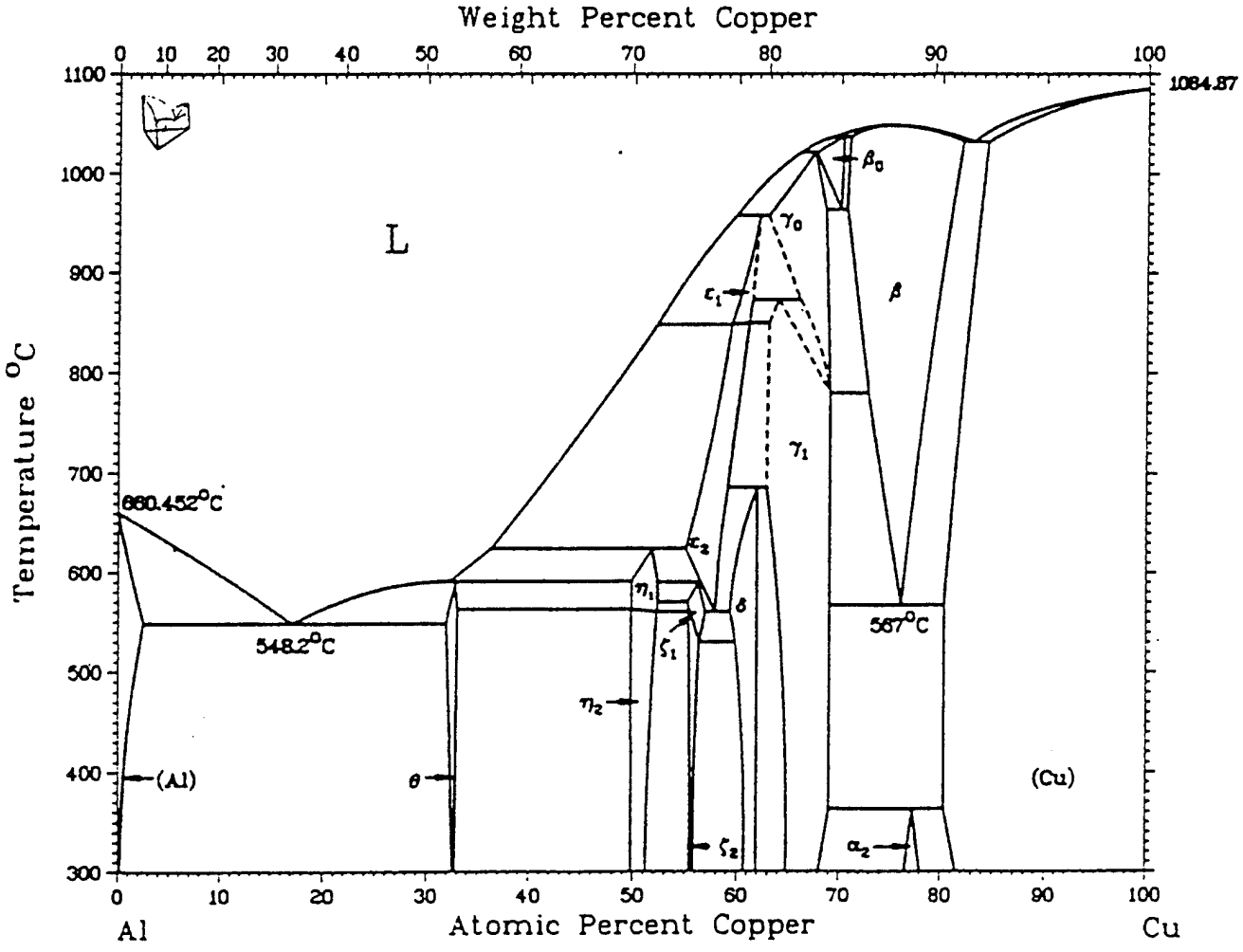

Figure 2.1: Al-Cu Phase Diagram From Ref. [14].

Al 2519 derives most of its strength through precipitation hardening. As the alloy cools from higher temperatures the copper in solution tends to precipitate out of the parent α phase [Ref. 16]. If the material is rapidly quenched, then the copper is trapped forming a supersaturated solid solution at room temperature. Subsequent aging at room temperature or higher will result in formation of new particles in the aluminum matrix. The (TTT) diagram in Figure 2.2 shows different metastable precipitates that form for various temperatures [Ref. 17]. The sequence as the alloy is slowly cooled is as follows.

$$\textbf{Supersaturated } \alpha \longrightarrow \textbf{GP Zones} \longrightarrow \theta'' \longrightarrow \theta' \longrightarrow \theta\ (Al_2Cu)$$

The Al 2519 alloy has 6.0 wt. percent copper and this is greater than the 5.65 wt. percent that would allow transition to a homogeneous alpha phase. Hence some θ will remain insoluble even after long solutionizing treatments.

B. PARTICLE STIMULATED NUCLEATION THEORY (PSN)

Superplasticity can only occur if the material grain structure is refined sufficiently [Ref. 18][Ref. 19]. There are currently two methods in commercial use for inducing a superplastic response in aluminum. Supral requires the addition of 0.4 wt. percent Zr to a 6.0 wt. percent Cu, Al-Cu alloy. During processing the zirconium forms fine Al_3Zr precipitate particles with an average diameter of 10 to 100 nm. These particles help to prevent nucleation during TMP [Ref. 1]. The grain structure is refined via continuous recrystallization (CRX) during subsequent plastic deformation when forming and the fine Al_3Zr particles suppress grain growth. Recrystallization of the aluminum occurs with a resulting average grain size of 6.0 μm [Ref. 2].

The Rockwell method uses discontinuous recrystallization (DRX) to produce a superplastic material [Ref. 1]. Solution heat treating followed by a rapid quench dissolves the second phase producing a supersaturated solid solution. Overaging of the material is

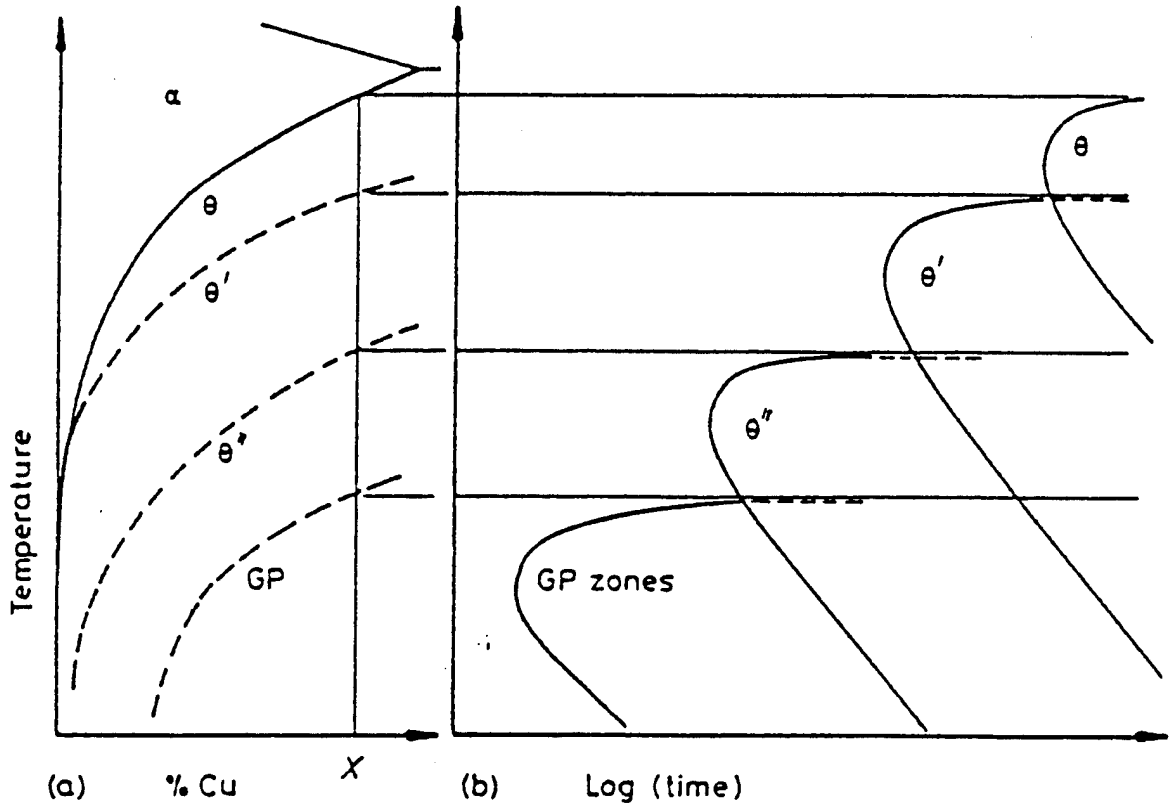

Figure 2.2: a) Al-Cu metastable phase solvus lines b) TTT curve showing the starting times for the various metastable phases of an aluminum copper alloy From Ref. [17].

then performed to produce evenly distributed particles with an average size large enough to support PSN of recrystallization. Warm rolling of the material induces a large strain energy concentration around the particles. Recrystallization begins when the material is subsequently reheated. Grain sizes on the order of 10 μm have been produced using this method. Particle size and dispersion are key elements in this process. [Ref. 20]

A dispersion of particles in a parent matrix can induce grain refinement of a coarse grained material via recrystallization if the particles do not deform as readily as the matrix when strain is imparted. For sufficiently large non-deforming particles local lattice rotations occur in the strained region surrounding these particles [Ref. 21]. These lattice rotations are found in association with cellular dislocation structures formed around particles of size $0.1 \geq$ μm. The overall dislocation density, ρ_g, can be estimated according to equation (1) [Ref. 22]:

$$\rho_g = \frac{8 f \cdot \gamma}{b d_p} \tag{1}$$

Where f equals the volume fraction, γ the shear strain, b the associated Burger's vector and d_p the particle diameter. Not all particles induce lattice rotations. If the particle diameter is less than 0.1 μm or there is a very low strain, the dislocations induced form prismatic loops that do not provide lattice rotations. Lattice reorientation is a prerequisite for recrystallization and so particles with a size of 0.1 μm and greater, and high strains, do promote PSN [Ref. 21]. Other factors must exist though because PSN has been observed mostly for particle diameters greater than 1.0 μm.

During straining the size of the deformation zone may be estimated using the strain hardening characteristics of the materials shown in equation (2):[Ref. 22]

$$\lambda = A d_p \varepsilon^{\frac{n}{n+1}} \tag{2}$$

Where λ equals the width of deformation zone, A is a material constant, ε the true axial strain and n the strain hardening coefficient from Holloman's equation,

$$\sigma = k\varepsilon^{n} \tag{3}$$

where σ equals the true stress. Inside the deformation zone, the rotated structures which form are termed embryos. These embryos may form new grains but two criteria must be met. First, there must be sufficient energy or sufficient size to be a viable nucleus capable of growth into the surrounding matrix: [Ref. 23]

$$\delta_{crit} = \frac{4\Gamma}{E} \tag{4}$$

where δ equals the critical size of an embryo, E the stored strain energy due to deformation and Γ the grain boundary interfacial energy. Second, the embryo size must be smaller than the deformation zone ($\delta_{crit} < \lambda$) [Ref. 24]. The combination of these two criteria leads to a relationship between particle size and strain for PSN. If $\delta_{crit} = \lambda$, then:

$$A \cdot d_{p,crit} \cdot \varepsilon^{\frac{n}{n+1}} = \frac{4 \cdot \Gamma}{E} \tag{5}$$

or

$$d_{p,crit} = \frac{4 \cdot \Gamma}{A \cdot E} \cdot \frac{1}{\varepsilon^{\frac{n}{n+1}}} \tag{6}$$

Thus d_p the particle size is inversely related to the strain, ε. This is illustrated schematically in Fig 2.3 [Ref. 25]. An estimate of the grain size associated with a certain

particle size may be made if the embryos all grow successfully until they impinge. The grain size will be approximately equal to the particle spacing D_s: [Ref. 25]

$$D_g \approx D_s \approx \frac{d_p}{f^{\frac{1}{3}}} \tag{7}$$

Here the particles are all assumed to have a size d_p which is greater than or equal to $d_{p,crit}$.

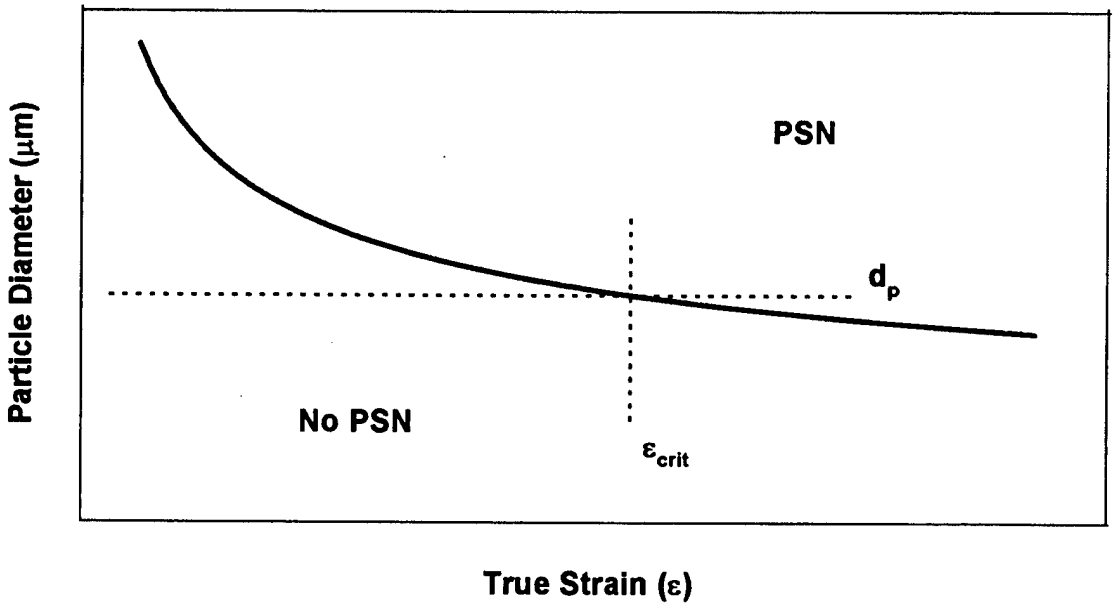

Figure 2.3 Shows the relationship between particle size and true strain. In order for PSN to occur for a given particle size the true strain must exceed ε_{crit}. From Ref. [25].

III. EXPERIMENTAL PROCEDURE

A. MATERIAL

The Aluminum alloy material used in this thesis was obtained from the ALCOA Technical Center, ALCOA Center, Pennsylvania. This alloy, designated 2519, was received in the form of a rolled plate 0.902 in (22.9 mm) thick and tempered to the T87 condition. The T87 treatment requires that the material be solution heat treated at 535°C, cold rolled by seven percent and then artificially aged for 24 hours at 165°C [Ref. 26].

The composition as provided by ALCOA is listed in Table 3.1.

TABLE 3.1: ALUMINUM 2519 COMPOSITION (WEIGHT PERCENT)

Cu	Mn	Mg	Fe	Zr	V	Si	Ti	Zn	Ni	Be	B	Al
6.06	0.30	0.21	0.16	0.13	0.04	0.07	0.06	0.03	0.01	0.002	0.001	bal

B. PROCESSING

Initial processing was performed by Zohorsky [Ref. 11] in previous research, although more material was produced in this study by the same procedures (which are described below). Sections were cut from the as-received plate with the longest dimension being in the previous rolling direction. The average size was 2.4 X 1.5 X 0.902 in (61 X 38.1 X 22.9 mm).

The thermomechanical processing of the aluminum consisted of five steps as summarized in Table 3.2. First, all samples were solution heat treated at 535°C for 100 minutes and then quenched. Then, a 9.8% prestrain was induced by rolling the samples at room temperature in a rolling mill. Final thickness after one pass was 0.819 in (20.8 mm). Initial overaging of all samples was subsequently conducted at 200°C for 50 hours. The

second phase of overaging was performed differently for each piece. Second stage temperatures were 350, 400 and 450°C and time at temperature was either 50 or 100 hours. All samples were furnace cooled to 200°C and then quenched to ambient (see Figure 3.1). Finally, rolling was completed in nine passes at 200°C (see Table 3.2). The final thickness was between 0.090 and 0.100 in (2.3 to 2.5 mm). A Fenn laboratory mill with 4.0 in. (102 mm) diameter rolls was employed in the rolling.

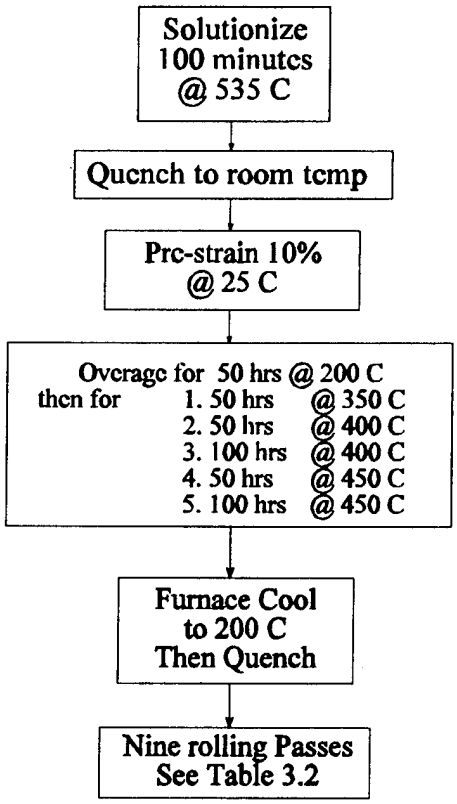

Figure 3.2: Thermomechanical Processing Steps

TABLE 3.3: ROLLING SCHEDULE

Roll Pass #	Initial Thickness (in)	Mill Gap Setting (in)	Final Thickness (in)	Mill Deflection (in)	True Strain	Strain Rate (1/sec)
1	0.819	0.742	0.767	0.025	0.066	0.832
2	0.767	0.657	0.685	0.028	0.113	1.135
3	0.685	0.580	0.607	0.027	0.121	1.243
4	0.607	0.513	0.541	0.028	0.115	1.288
5	0.541	0.432	0.460	0.028	0.162	1.628
6	0.460	0.339	0.372	0.033	0.212	2.033
7	0.372	0.228	0.234	0.006	0.464	3.438
8	0.234	0.122	0.162	0.040	0.368	3.819
9	0.162	0.045	0.090	0.045	0.588	5.948

C. TENSILE TESTING

Specimens were cut from the as-rolled sheet and milled to a gage length of 0.5 in (12.7 mm) as shown in Figure 3.4. Tensile testing was performed on an Instron machine with a five-zone, clam-shell furnace around the test area. Temperatures were controlled to within ±1°C over the test area which consisted of the middle three zones of the furnace. Tensile tests were conducted at constant strain rates of 10^{-2}, 10^{-3} and 10^{-4} sec^{-1} while test temperatures were 300, 350, 400 and 450°C. All specimens were quenched to ambient just after fracture occurred.

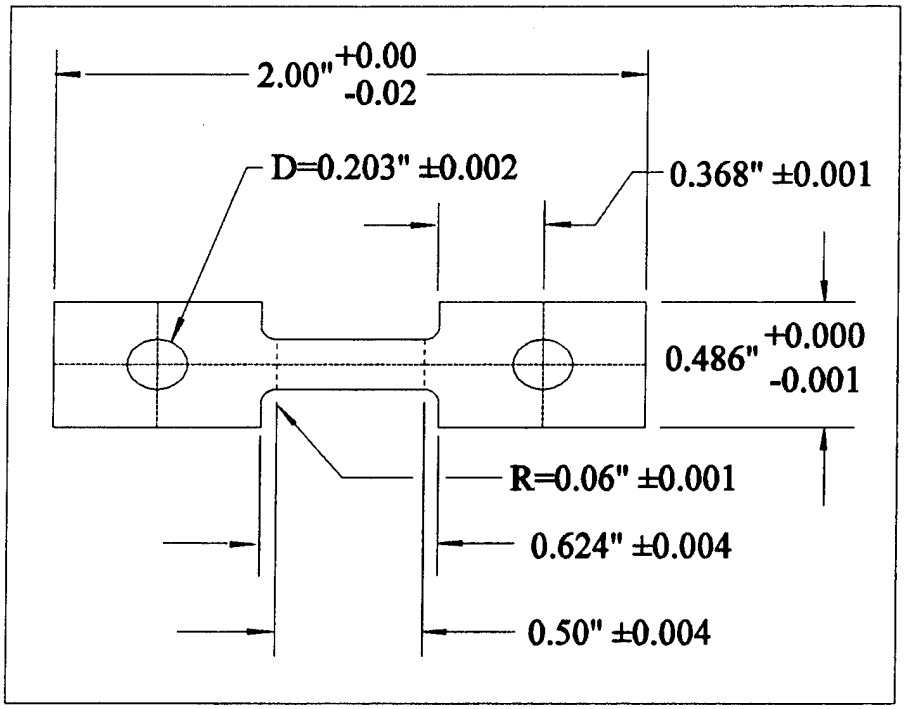

Figure 3.4 Tensile Test Specimen Schematic

D. METALLOGRAPHIC SAMPLE PREPARATION

Tested samples were sectioned parallel to the tensile axis using a Buehler Isomet low speed diamond saw with Buehler Isocut oil based lubricant. The cut surface was then ground using a Struers Knuth-Rotor 3 grinder. Silicon carbide paper was used with grits of 800, 1000, 2400 and 4000P. Each sample was held with moderate pressure on successive paper grits for 30 seconds each. Polishing was performed on 12 inch diameter Buehler wheels rotating at 400 RPM. Six-micron diamond compound was used on Bueler MICROCLOTH polishing cloth. Both 1.0 and 0.25 micron diamond compounds were used on Buehler CHEMOMET cloth. All polishing was performed with Struers DP green alcohol based lubricant. Polishing was done with moderate to light pressure for 30 seconds on each wheel.

Electropolishing was performed on all samples. A solution of 30 percent nitric acid and 70 percent methanol was cooled to -20°C in a stainless steel beaker. The cooling was done by immersing the beaker in an insulated bath which contained liquid nitrogen cooled methanol. Temperatures were measured in both the bath and polishing solution prior to electropolishing. Samples were coated with a non conductive lacquer where polishing was not desired and then immersed into the beaker. Polishing was done at 7.0 volts for 2 minutes with the polishing acid being magnetically stirred and the sample acting as the anode. Samples were rinsed using ethanol and dried immediately.

E. MICROSCOPY

Samples were examined in an SEM operating in backscatter mode with accelerating voltages of either 5.0 KV or 20 KV. Photographs taken at 5.0 KV accelerating voltage were intended to reveal the aluminum grain structure. Contrast was adjusted to resolve the grains by enhancing channeling contrast. The θ particles were evident and these micrographs were also used to determine the volume fraction of the second phase as well. Micrographs taken at 20 KV were used to examine the θ particles at higher resolution. All micrographs were taken at similar working distances and magnifications to facilitate comparison later.

F. IMAGE ANALYSIS

Micrographs were scanned into a personal computer and were analyzed using Image-Pro Plus 1.2 for Windows. The data collected was to access the volume fraction and average diameter of the θ particles. Linear intercept methods were used to ascertain the average aluminum grain diameter. Matlab and Excel 5.0 were used to produce the plots and histograms.

IV. RESULTS AND DISCUSSION

A. TENSILE TEST RESULTS

Table 4.1 lists the results of the tensile testing of this research. Each different test is delineated by strain rate and then test temperature. For each testing condition, five TMPs are listed by increasing overaging temperature and time. Not all TMPs were evaluated for all conditions listed; this is denoted by a "/" in the table. Testing was not done in these areas because of a shortage of samples due to the small amount of rolled material for each process and cracks produced during the rolling. Some conditions were tested twice due to irregularities during testing and these rows are marked "repeat".

Table 4.1: Results of all Superplastic testing

Strain Rate	TMP		Test Temperature							
			300 °C		350 °C		400 °C		450 °C	
	Temp	Time	elongation	max stress	elongation	max stress	elongation	max stress	elongation	max stress
sec^{-1}	°C	hours	%	σ MPA	%	σ MPA	%	σ MPA	%	σ MPA
10^{-2}	350	50	99.2	87.5	150.9	48.5	165.8	33.8	151.3	25.2
	400	50	110.6	82.0	137.2	48.0	187.6	30.6	157.6	23.7
repeat ⇨	400	50	98.4	87.8						
	400	100	99.0	83.9	123.5	44.5	139.7	32.0	186.0	23.7
	450	50	/	/	/	/	/	/	/	/
	450	100	/	/	127.9	43.3	133.9	32.3	166.5	24.7
10^{-3}	350	50	141.6	53.0	213.1	28.5	196.1	20.3	128.7	16.6
	400	50	140.6	50.8	257.3	30.7	195.8	17.7	178.5	14.7
repeat ⇨	400	50	153.3	48.7						
	400	100	153.6	52.9	187.5	28.4	188.2	19.3	156.2	14.5
	450	50	129.2	46.6	170.2	27.0	225.8	19.7	/	/
	450	100	101.5	52.8	147.3	30.3	158.6	19.8	/	/
10^{-4}	350	50	171.1	31.8	213.2	14.7	112.2	13.2	87.1	11.4
	400	50	204.7	29.4	226.4	16.3	183.6	10.8	190.1	6.9
	400	100	162.2	31.4	162.9	17.3	168.4	12.0	218.9	8.2
	450	50	168.2	29.9	241.6	16.4	266.4	9.5	/	/
repeat ⇨	450	50					250.1	9.8		
	450	100	43.3	31.3	170.0	18.6	196.3	11.7	293.4	6.0

The shading of test entries in areas of Figure 4.1 indicate that microscopy and grain size analysis was performed on that particular sample.

Stress strain curves typical of superplastic flow were observed. Three representative plots are shown superimposed in appendix A. The samples were all tested at the same temperature, 400°C, but strain rates were 10^{-2}, 10^{-3} and 10^{-4} sec^{-1}, respectively. Higher maximum stresses were observed at higher strain rates and this corresponded with lower overall elongation. The lowest strain rate of 10^{-4} sec^{-1} was seen to have the greatest ductility; this trend can be seen in the graphs provided in appendix B, showing strain rate versus percent elongation for each separate TMP tested.

In examining the data, it was found that the maximum elongation also tended to occur at a test temperature equal to the final overaging temperature in prior TMP of the specimen tested. This can be seen in Figures 4.2 thru 4.4b. This trend is apparent for all but one of the TMPs investigated.

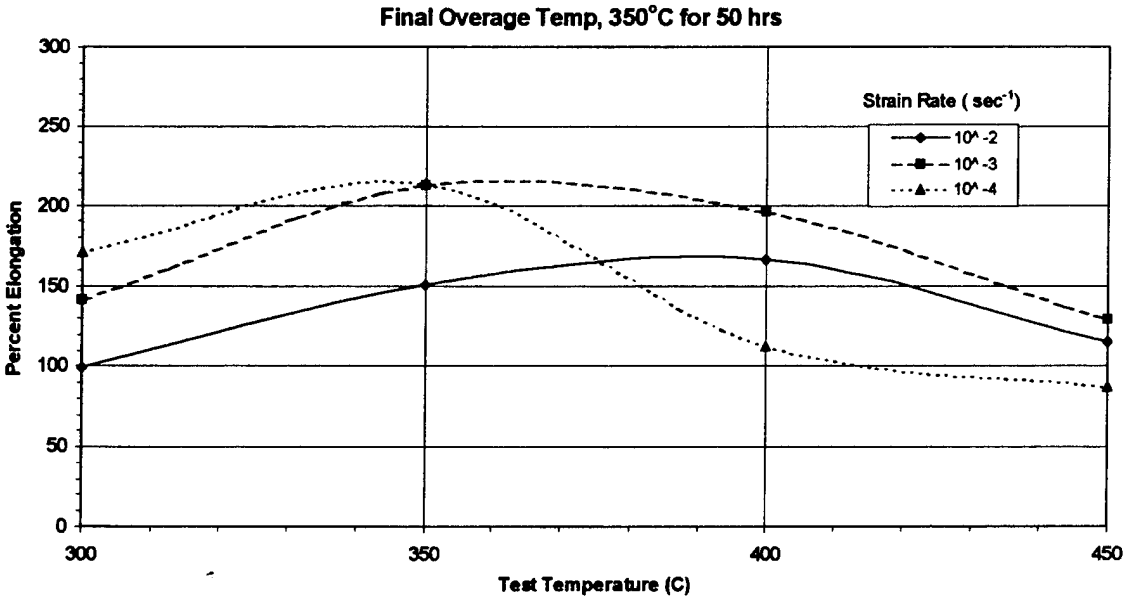

Figure 4.2 Test temperature vs. elongation for a final overaging temperature of 350°C and 50 hours.

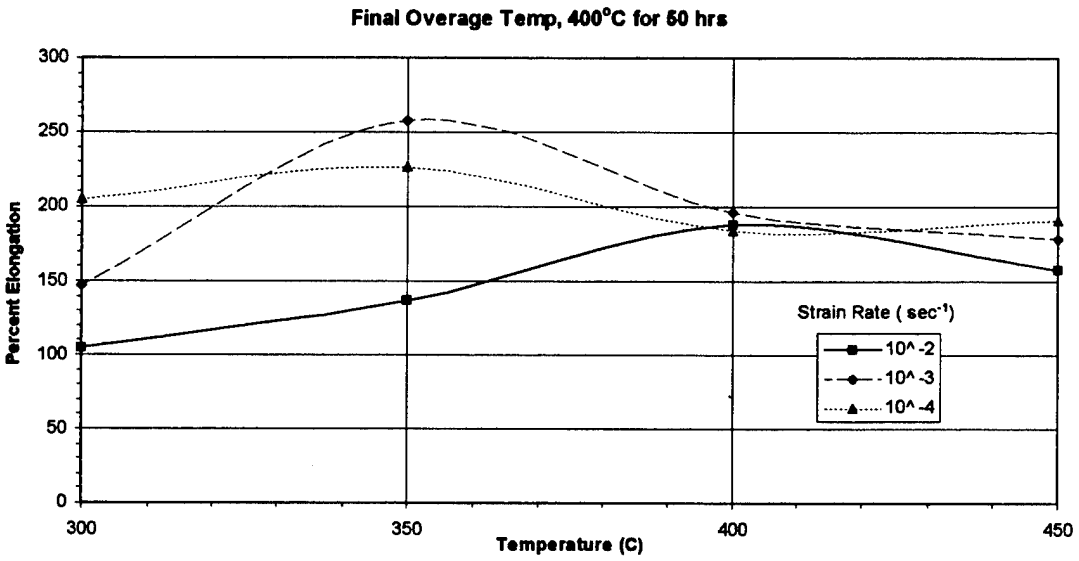

Figure 4.3a Test temperature vs. elongation for a final overaging temperature of 400°C and 50 hours..

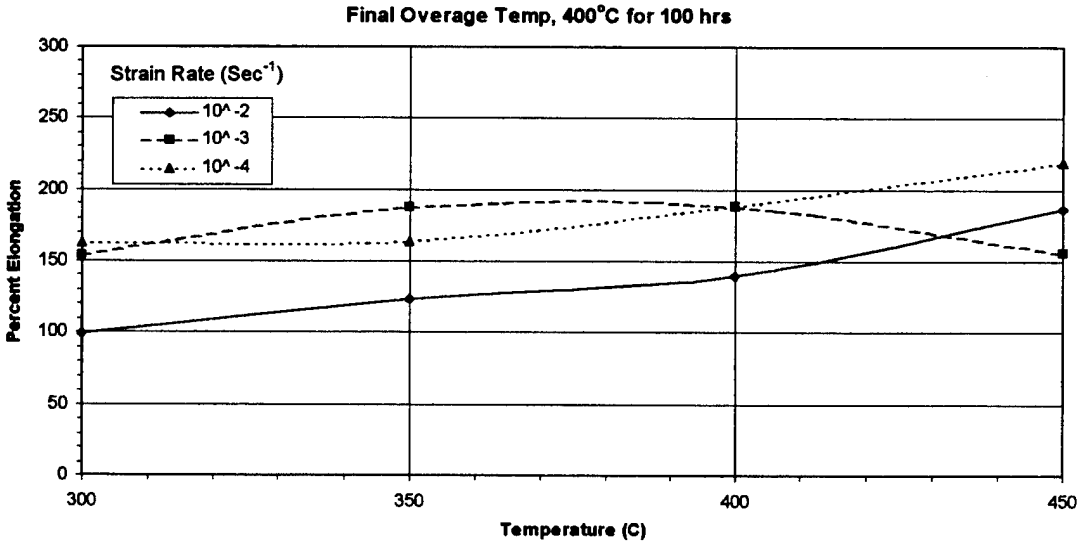

Figure 4.3b Test temperature vs. elongation for a final overaging temperature of 400°C and 100 hours.

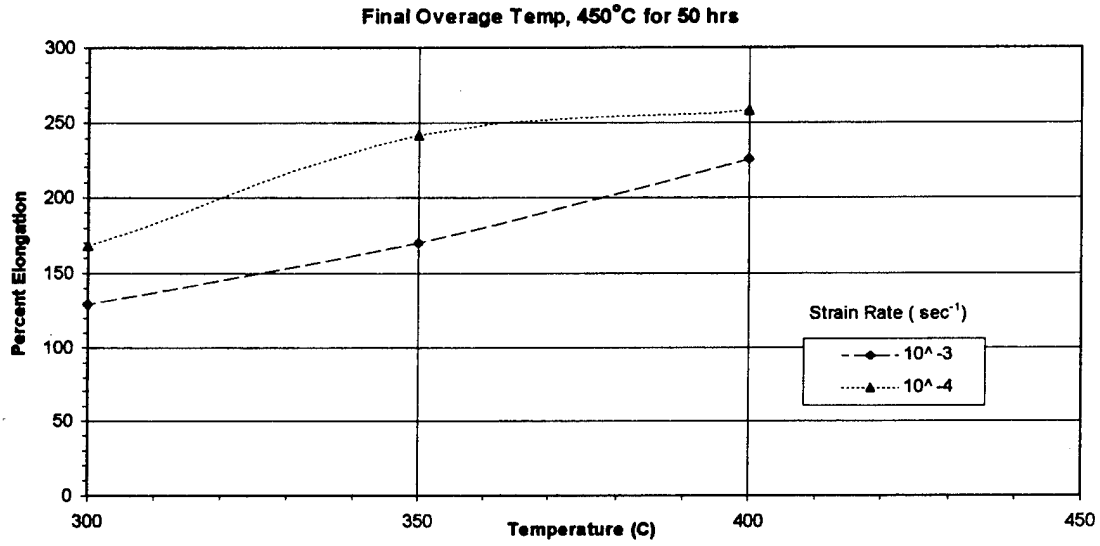

Figure 4.4a Test temperature vs. elongation for a final overaging temperature of 450°C and 50 hours

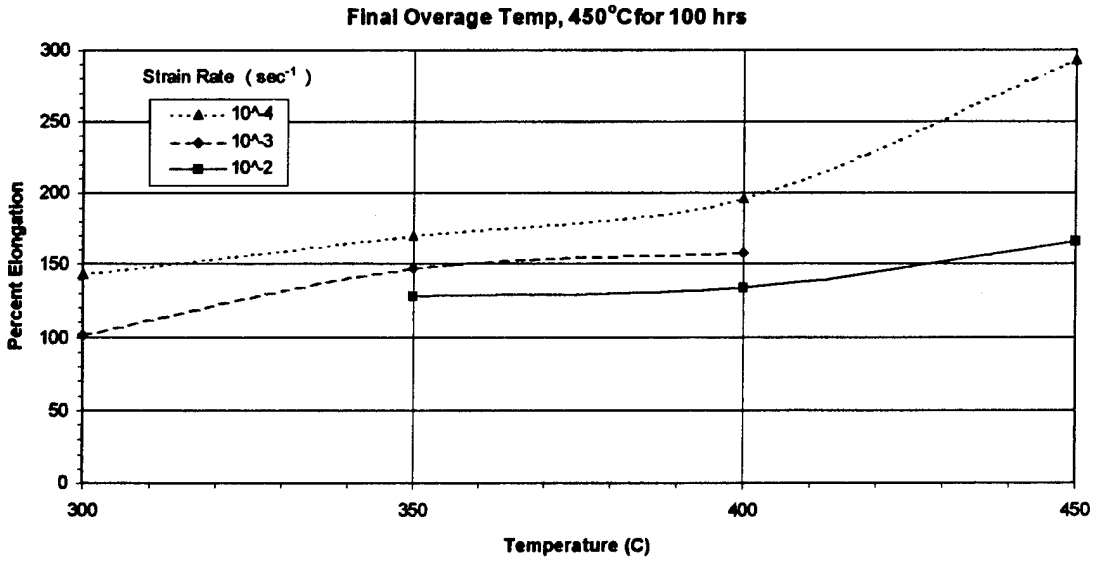

Figure 4.4b Test temperature vs. elongation for a final overaging temperature of 450°C and 100 hours.

B. MICROSCOPY RESULTS

All micrographs are oriented with the rolling and tensile test direction from left to right in the field of view. Figure 4.5a shows a backscattered electron micrograph of the as-received Al 2519. The aluminum grains are clearly visible when a low accelerating voltage is used to enhance the channeling contrast. Average grain size as measured by the mean linear intercept method (MLI) and corrected to a true volume grain size by the relation d = 1.776*(MLI) is 57.3μm. The grains show elongation due to rolling. Figure 4.5b shows the same material but at both a higher magnification and accelerating voltage to show the θ particles. In both micrographs, θ particles clearly exhibit cracking. This likely is due to the rolling in original manufacture and indicates that the θ particles are less deformable than the aluminum grains. It should be noted that the θ particles are elongated in the direction of rolling.

Figure 4.5.a Backscattered electron micrograph of the as received aluminum 2519, showing the aluminum grain structure

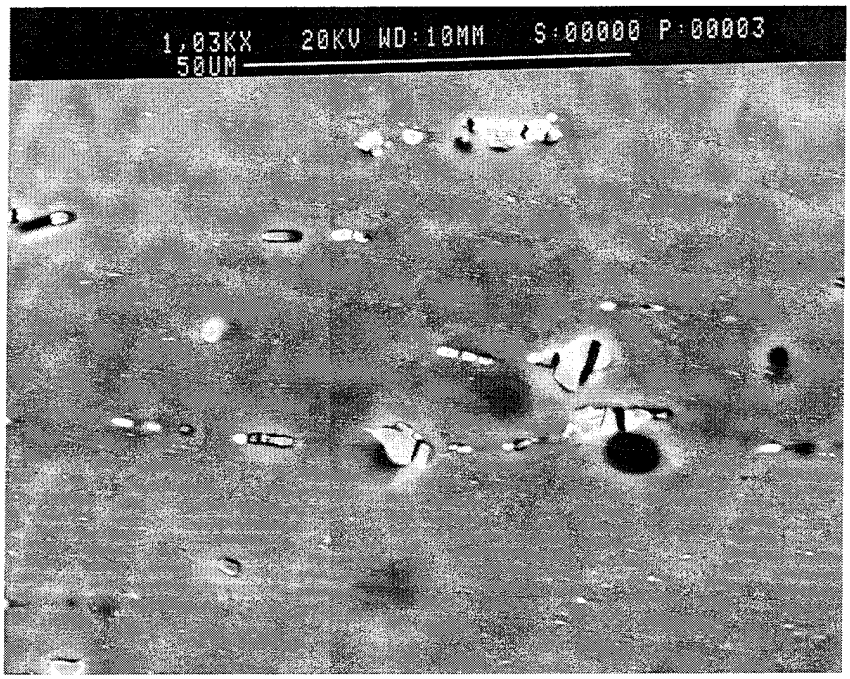

Figure 4.5.b Backscattered electron micrograph of the as received aluminum 2519, showing the θ precipitates at high magnification.

Figure 4.6 shows material from a rolled but untested TMP involving overaging at 400°C for 50 hours. This micrograph suggests a high volume fraction of θ. Unfortunately, volume fraction calculations were not accurate and this will be discussed later. A fine dispersion of particles is evident but a few large particles are still seen. Channeling contrast at lower voltages was not evident in material when examined in an as-rolled condition.. This was due to the high dislocation density and associated lattice curvature left at the conclusion of the rolling procedure. Figure 4.7a shows the grip section of a sample tested at 350°C an 10^{-3} sec^{-1} strain rate; overaging had been accomplished at 400°C for 50 hours. The aluminum grain structure is now clearly evident; grains are elongated in the prior rolling direction and further grain elongation is apparent after tension testing (Fig 4.7b). Average grain size was measured to be 26.1μm for the

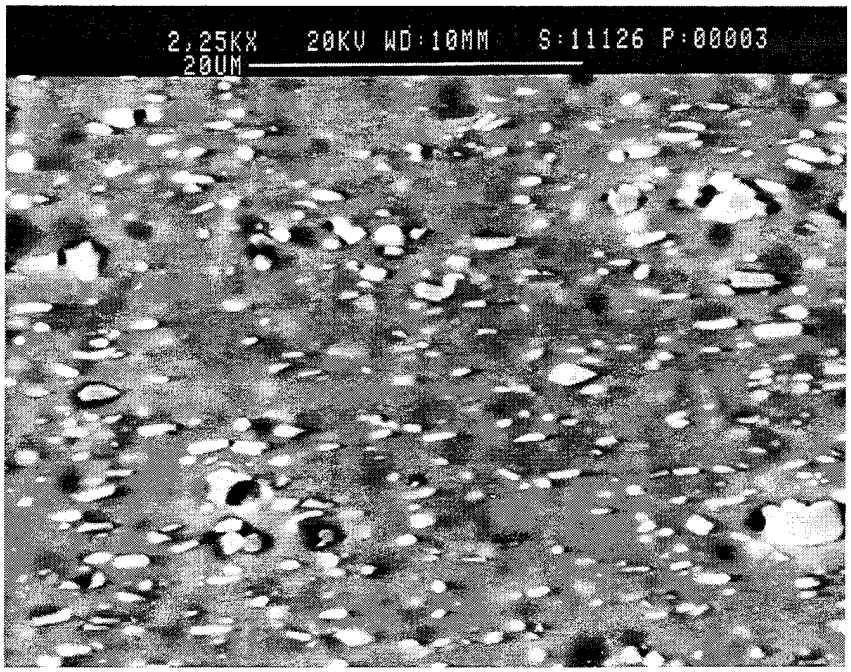

Figure 4.6 Backscattered electron micrograph of a rolled but not tested sample overaged at 400°C for 50 hours.

as-rolled and annealed material. Careful examination of the microstructure in the deformed gage section shows that all grains are elongated but also show signs of breaking up into finer recrystallized grains . The specimen elongated to 257.3% and exhibited a quasi brittle fracture surface indicative of cavity formation.

Figures 4.8 thru 4.11 show the grip sections of samples which had all been overaged at 450°C for 100 hours and tested at a strain rate of 10^{-4} sec^{-1} utilizing test temperatures of 300, 350, 400 or 450°C. Figure 4.8 shows the microstructure of a sample tested at 300°C and suggests no recrystallization; large, elongated grains and elongated θ particles are evident throughout the sample. Average grain size, however, is 19.7 μm. The micrograph in Figure 4.9 was obtained from a sample tested at 350°C and shows some evidence of recrystallization. Grain size was measured at 18.5μm. Elongations were low; 143.3 % for the sample of Figure 4.8 to 170% for that of Figure

4.9. Figure 4.10 exhibits the finest grain size produced in this study in which an average diameter of 11.2 μm was obtained. These grains appear to be fully recrystallized and are equiaxed in shape. Large θ particles are often seen to be at the junction of three or more grains, supporting the role of particles in recrystallization according to PSN theory. The formation of one or more new grains at sufficiently large particles and their growth might be expected to produce the structure shown in Figures 4.10 and 4.11. Elongation of 196.3% was achieved for the sample of Figure 4.10. The sample of Figure 4.11 produced the greatest elongation in this study, 293.4%. The microstructures in Figures 4.10 and 4.11 are similar except that the grain size is larger in the material heated and tested at 450°C (Figure 4.11) reflecting greater grain growth at the higher temperature. The measured grain size was 17.4 μm for the micrograph of Figure 4.11.

The grain size is plotted versus test temperature for the previous four micrographs in Figure 4.12. The as-received material had a grain size of 57.3 μm and this is included. It is clear that processing was resulting in grain refinement down to 11.2 μm for the material tested at 400°C. It appears that the as-rolled structure recovers upon heating to temperatures of 350°C or below, with some evidence of recrystallization in deformed samples. Full static recrystallization is observed upon heating to 400°C; grain growth following recrystallization results in coarser material at still higher temperatures.

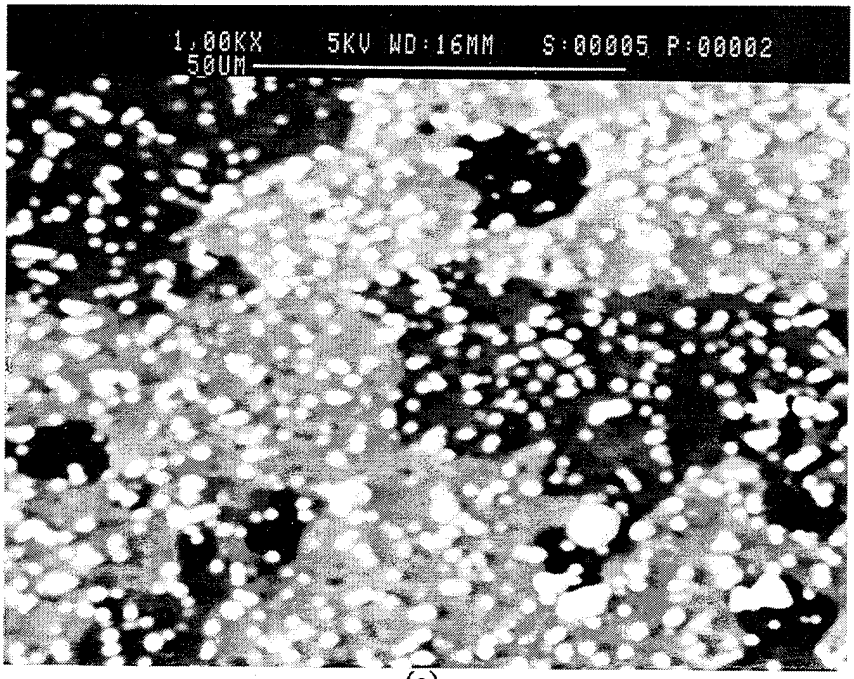

(a)

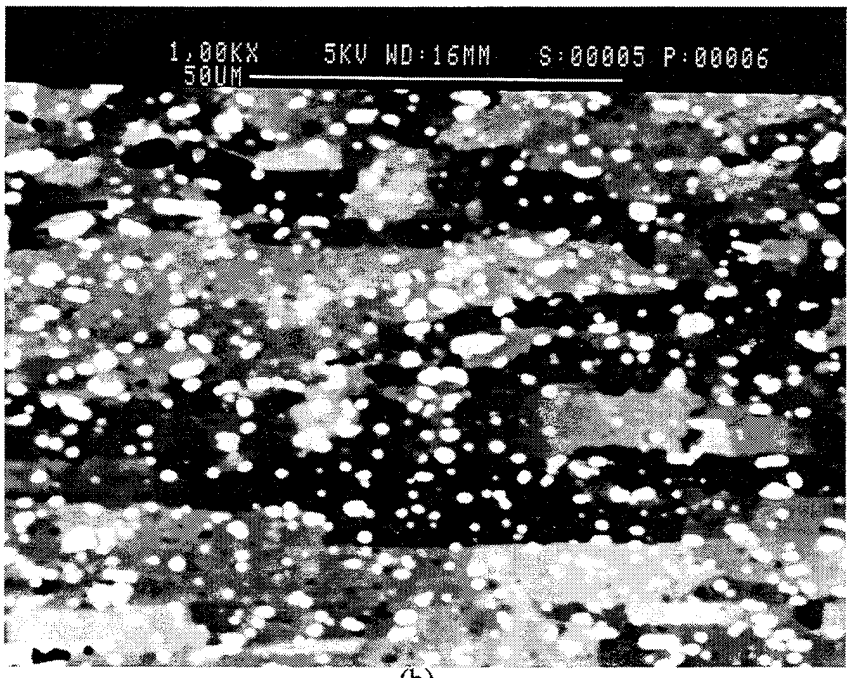

(b)

Figure 4.7 a&b Backscattered electron micrographs of a sample overaged at 400°C for 50 hours and then tested at 350°C with a strain rate of 10^{-3} $sec^{-1,}$ a) grip section b) gage section.

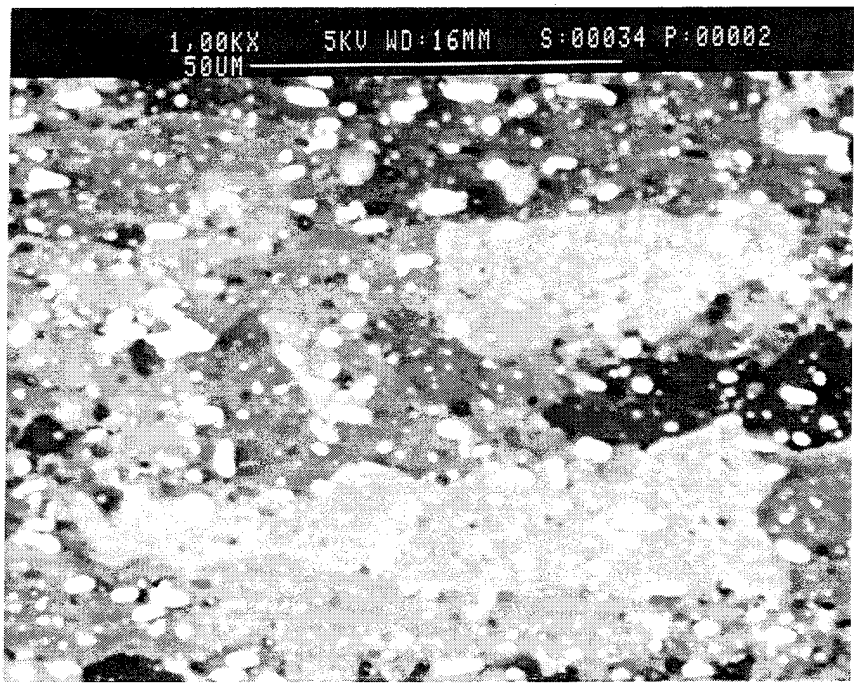

Figure 4.8 Backscattered electron micrograph of a sample overaged at 450°C for 100 hours and then tested at 300°C with a strain rate of 10^{-4} $sec^{-1,}$

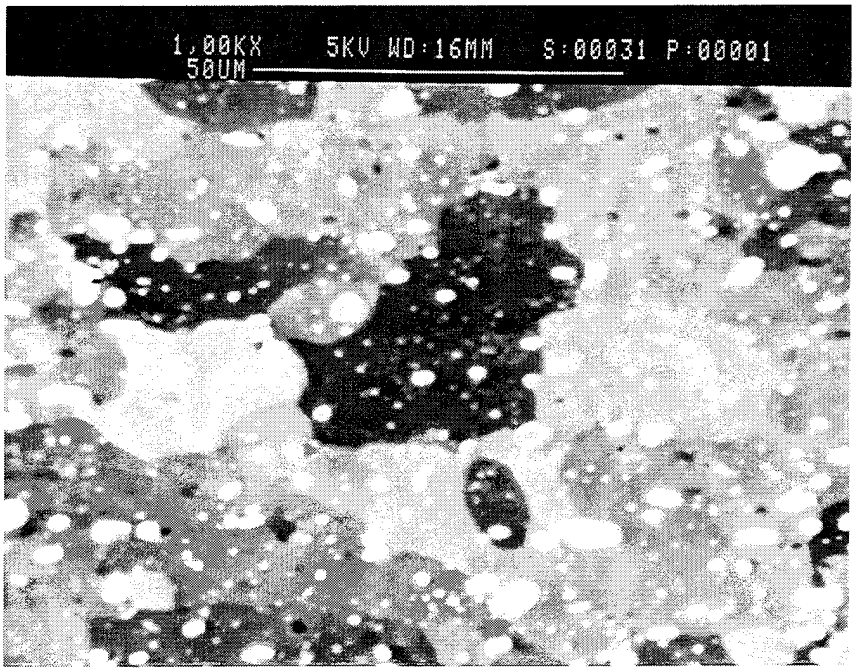

Figure 4.9 Backscattered electron micrograph of a sample overaged at 450°C for 100 hours and then tested at 350°C with a strain rate of 10^{-4} $sec^{-1,}$

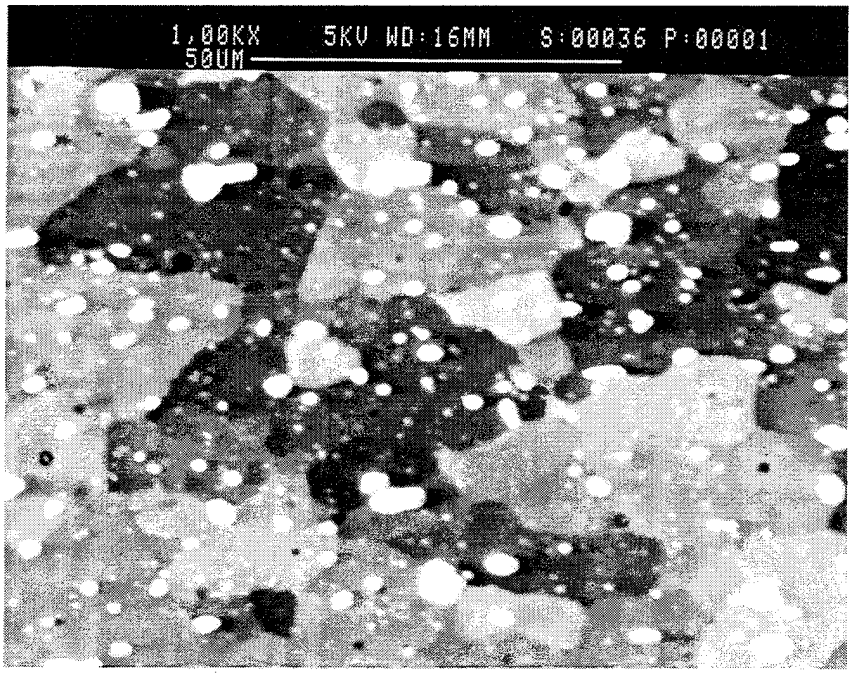

Figure 4.10 Backscattered electron micrograph of a sample overaged at 450°C for 100 hours and then tested at 400°C with a strain rate of 10^{-4} sec^{-1}.

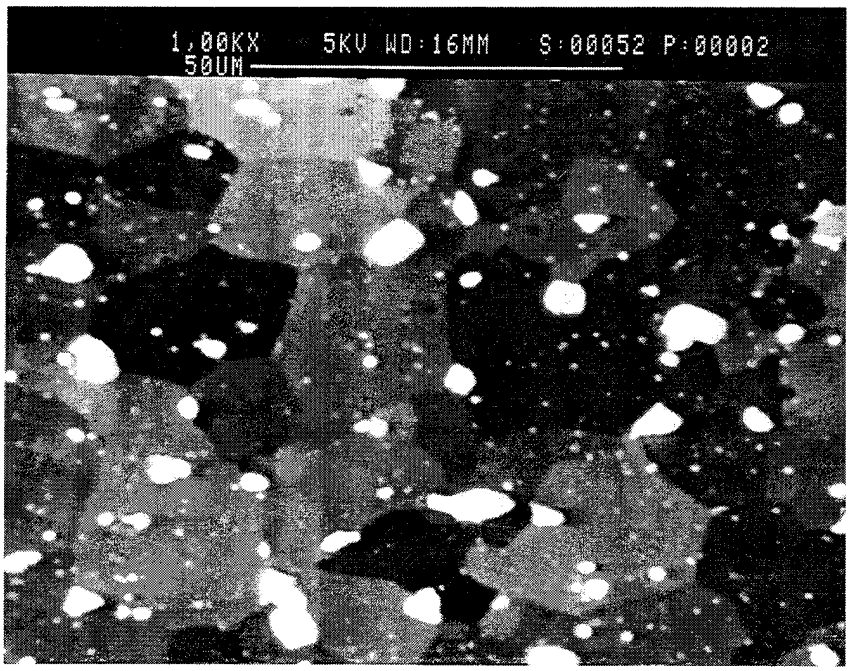

Figure 4.11 Backscattered electron micrograph of a sample overaged at 450°C for 100 hours and then tested at 450°C with a strain rate of 10^{-4} sec^{-1}.

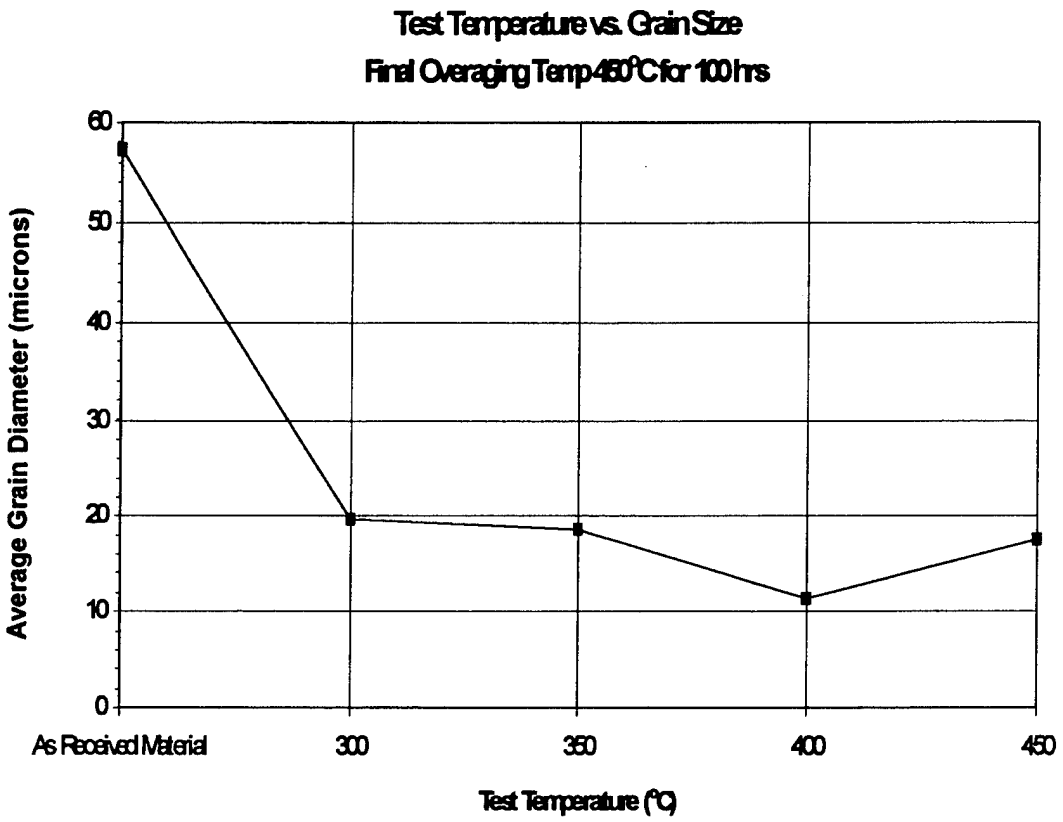

Figure 4.12 Test temperature versus average grain size for a material with a final overaging temperature of 450°C for 100 hours. All samples were tested at a strain rate of 10^{-4} sec^{-1}.

Figures 4.13 & 4.14 are micrographs of grip sections for material overaged at 450°C for 100 hours and tested at 400°C. Strain rates were 10^{-2} & 10^{-3} $sec^{-1,}$ respectively. These micrographs, along with that of Figure 4.10 show that recrystallization is essentially complete after 63 minutes (Figure 4.13) and that grain growth is minimal with prolonged heating. Essentially no changes are apparent when comparing Figure 4.14 (86 minutes at temperature) and Figure 4.10 (6.5 hours at temperature). Figure 4.15 summarizes this, trend starting with the grain size of the as-received material.

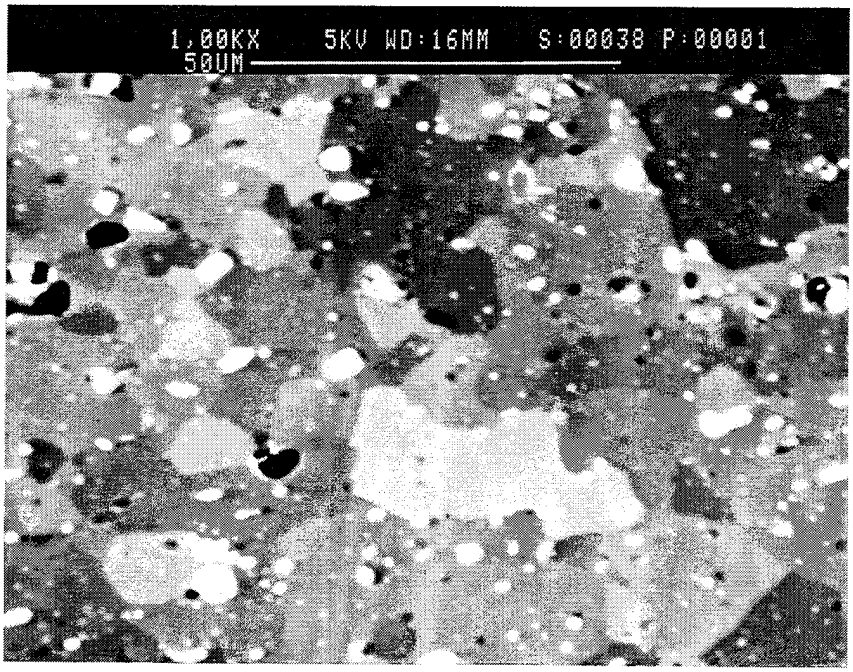

Figure 4.13 Backscattered electron micrograph of a sample overaged at 450°C for 100 hours then tested at 400°C with strain a rate of 10^{-2} sec^{-1}, grip section.

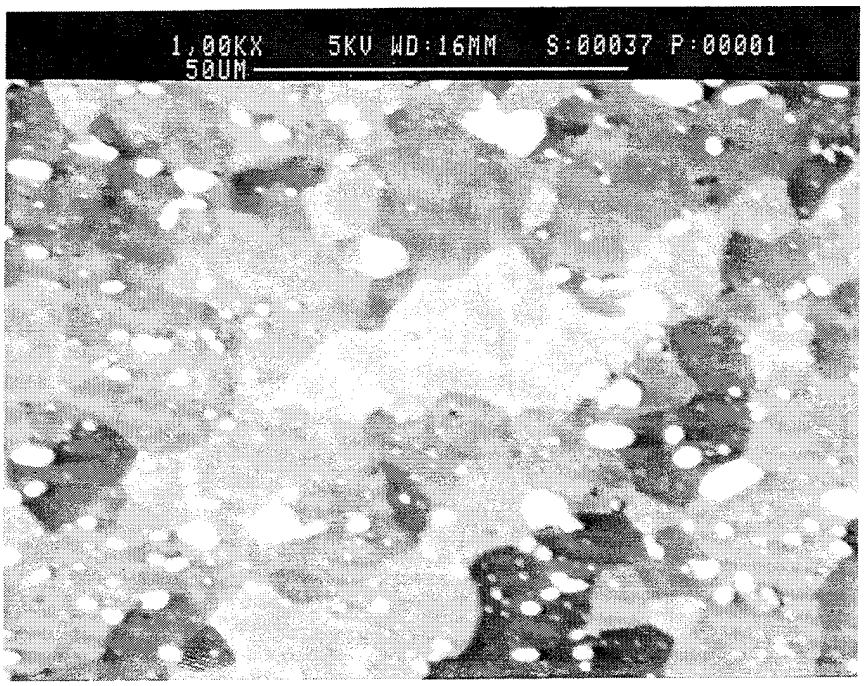

Figure 4.14 Backscattered electron micrograph of a sample overaged at 450°C for 100 hours then tested at 400°C with strain a rate of 10^{-3} sec^{-1}, grip section.

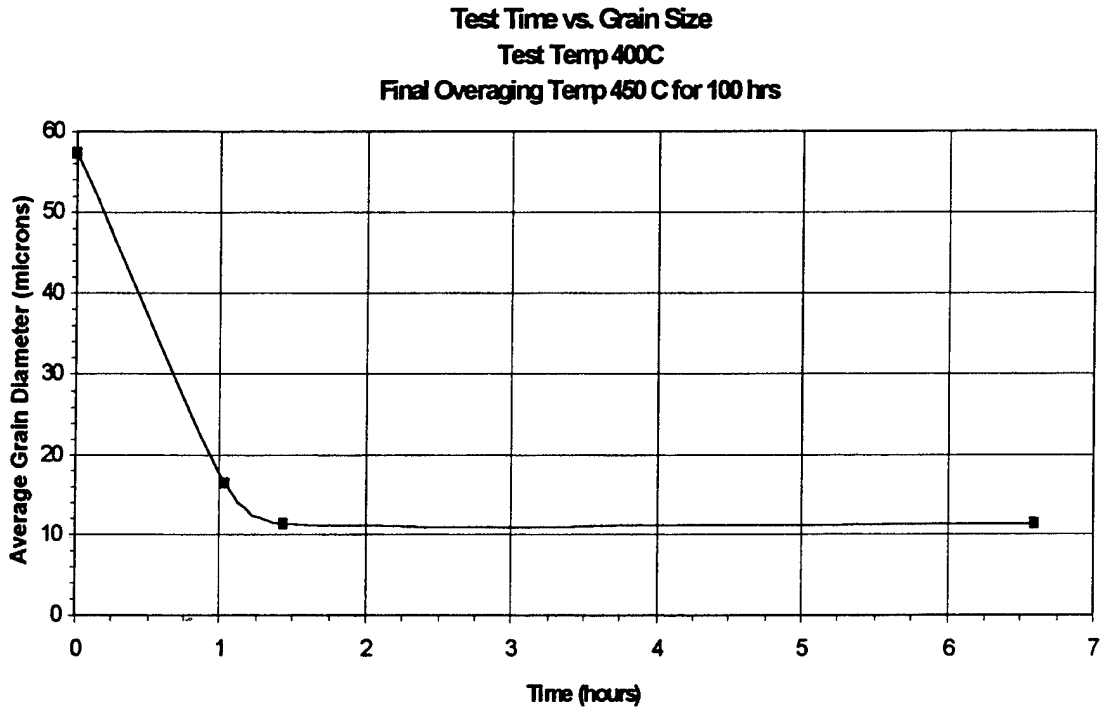

Figure 4.15 Test time versus grain size for samples tested at 400°C and strain rates from 10^{-2} to 10^{-4} sec^{-1}.

The grains tended to elongate further when deformed during testing in the case of materials that had not fully recrystallized. This can be seen in the micrographs of Figures 4.16 a&b. These show the gage sections, for material which had been overaged at 450°C for 100 hours, after testing at 350°C. Figure 4.16a is half way between the grip and the fracture surface while Figure 4.16b is just inside of the fracture surface. Comparison to Figure 4.9 (the grip section) reveals the elongation of the grains as the center of the gage section is approached. Figure 4.17 a&b show microstructures of the gage section corresponding to Figure 4.11 which had its final overaging temperature at 450°C for 100 hours. These micrographs show little or no elongation of the grains for material fully recrystallized and then deformed at a corresponding temperature where superplastic elongation has been achieved.

The retention of an equiaxed grain structure during straining suggests deformation by grain boundary sliding. This is generally recognized to be the mechanism of superplastic deformation. The formation of cavities on grain boundaries and at particle/matrix interfaces during grain boundary sliding is frequently observed. Here, extensive cavitation was seen in the deformed gage sections of the most ductile conditions (Figures 4.16 and 4.17); this is consistent with the observation of flat, i.e. quasi-brittle, fracture surfaces in spite of elongations approaching 300 percent. This also suggests that improved ductilities would be obtained with the use of superimposed hydrostatic pressure to suppress cavity formation.

Figures 4.18 thru 4.21 summarize the effects of TMP and subsequent heating on average grain size. All four micrographs are of grip sections of specimens tested at 400°C with a strain rate of 10-4 sec^{-1}. TMP conditions are listed with the micrographs. The effect of TMP parameters is shown in Figure 4.22 in a plot relating grain size to prior TMP conditions As overaging temperature is increased, the grain size obtained is reduced. Increased time at temperature has a small effect, however, on the grain size after

TMP. Only for materials overaged at 450°C is there any reduction in grain size as overaging time varies from 50 to 100 hours.

The relationship between TMP and the particle volume fraction and average diameter were evaluated and results are included in Figure 4.23. The volume fraction of θ is considerably in excess of that predicted by applying the lever rule to the phase diagram in Figure 2.1. This is evidently the result of electropolishing resulting in preferential removal of the aluminum matrix which allowed the θ to stand in relief. The equilibrium volume fraction at 450°C would be 0.048 (4.8 pct.) and only 0.07 (7.0 pct.) at room temperature. Efforts to change polishing conditions were unsuccessful.

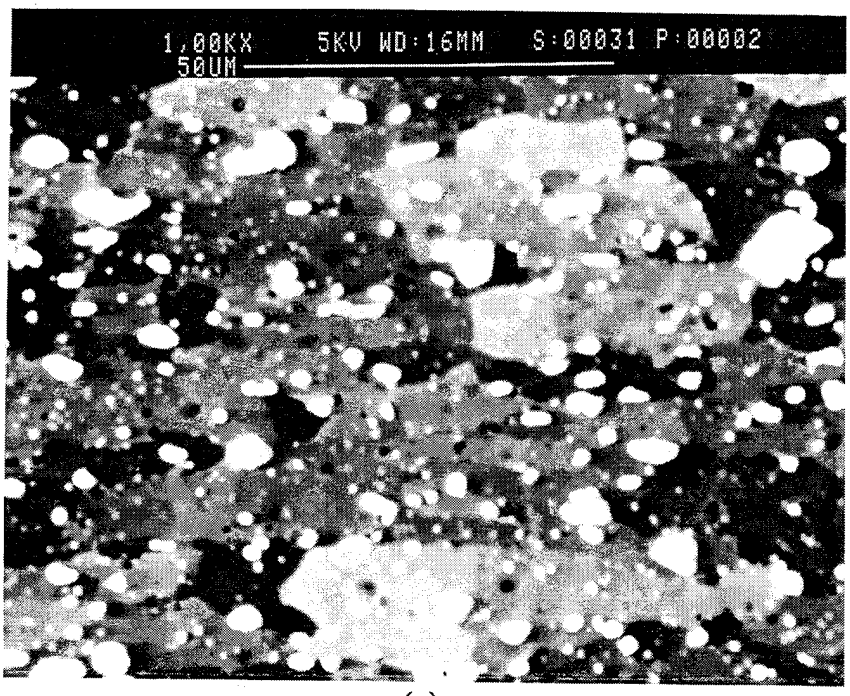

(a)

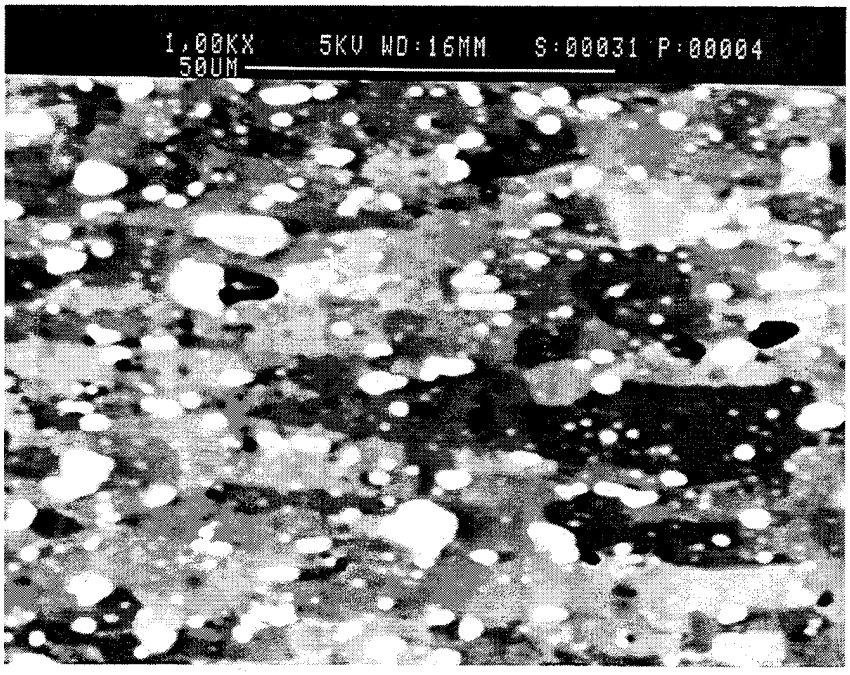

(b)

Figure 4.16 a&b Backscattered electron micrograph of a sample overaged at 450°C for 100 hours then tested at 350°C with strain a rate of 10^{-4} sec^{-1}, a) halfway down gage section b) next to fracture.

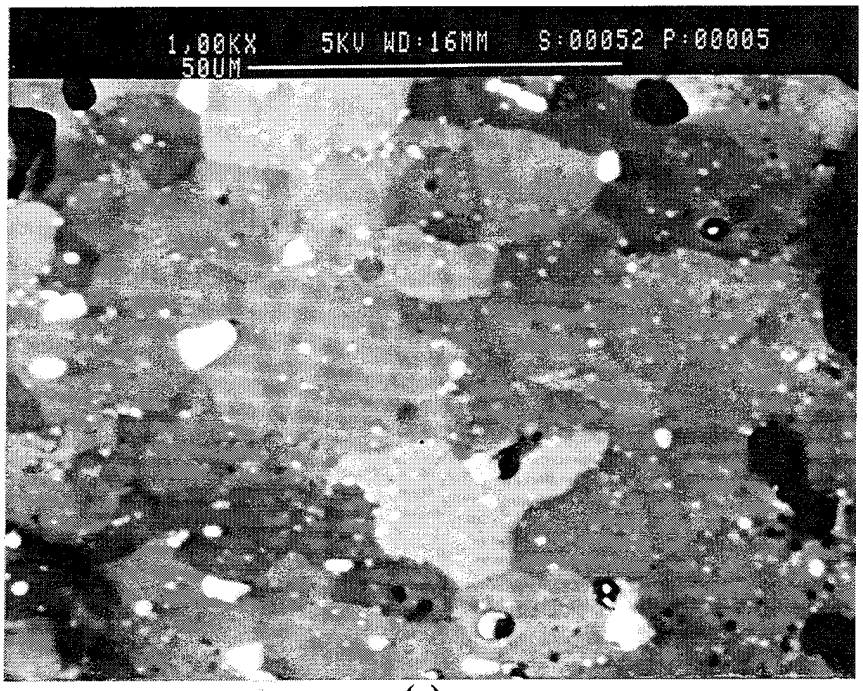

(a)

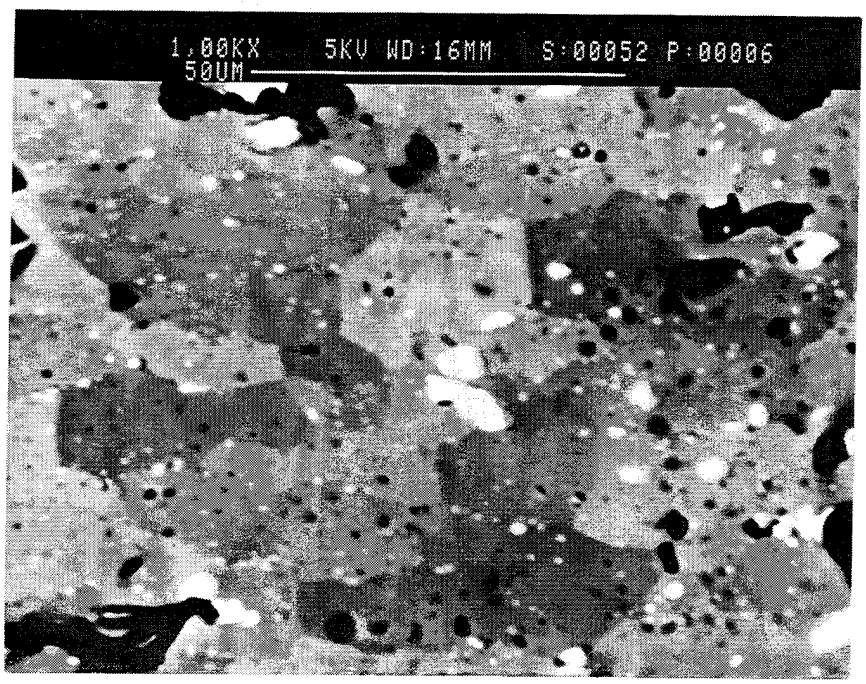

(b)

Figure 4.17 a&b Backscattered electron micrograph of a sample overaged at 450°C for 100 hours then tested at 450°C with strain a rate of 10^{-4} sec^{-1}, a) halfway down gage section b) next to fracture.

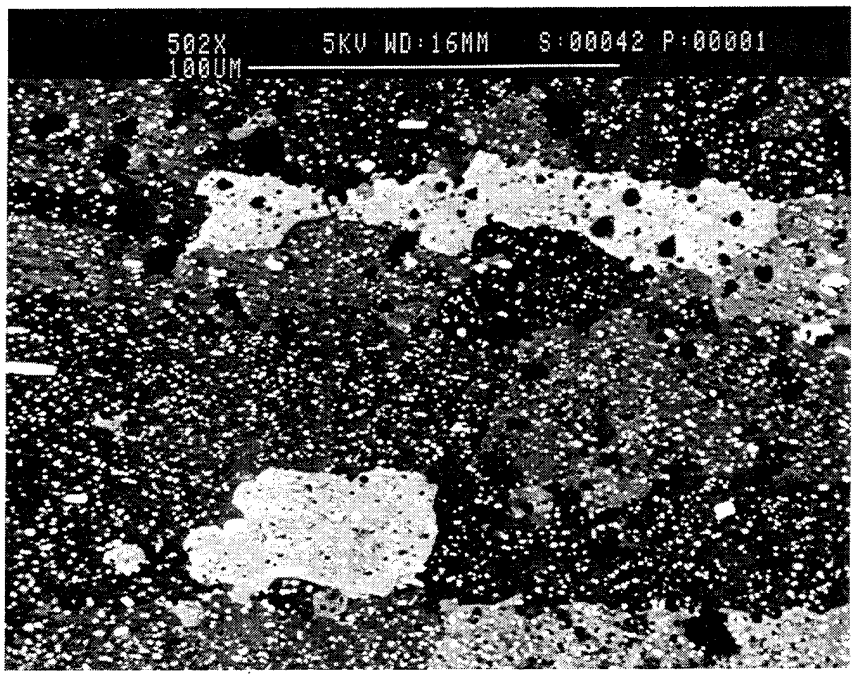

Figure 4.18 Backscattered electron micrograph of a sample overaged at 350°C for 50 hours then tested at 400°C with strain a rate of 10^{-4} sec^{-1}, grip section.

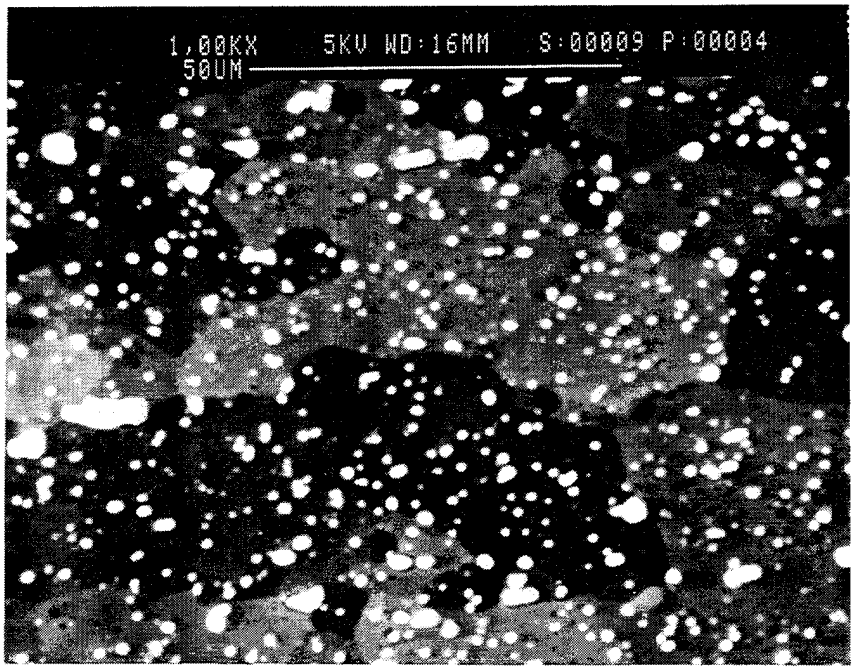

Figure 4.19 Backscattered electron micrograph of a sample overaged at 400°C for 50 hours then tested at 400°C with strain a rate of 10^{-4} sec^{-1}, grip section.

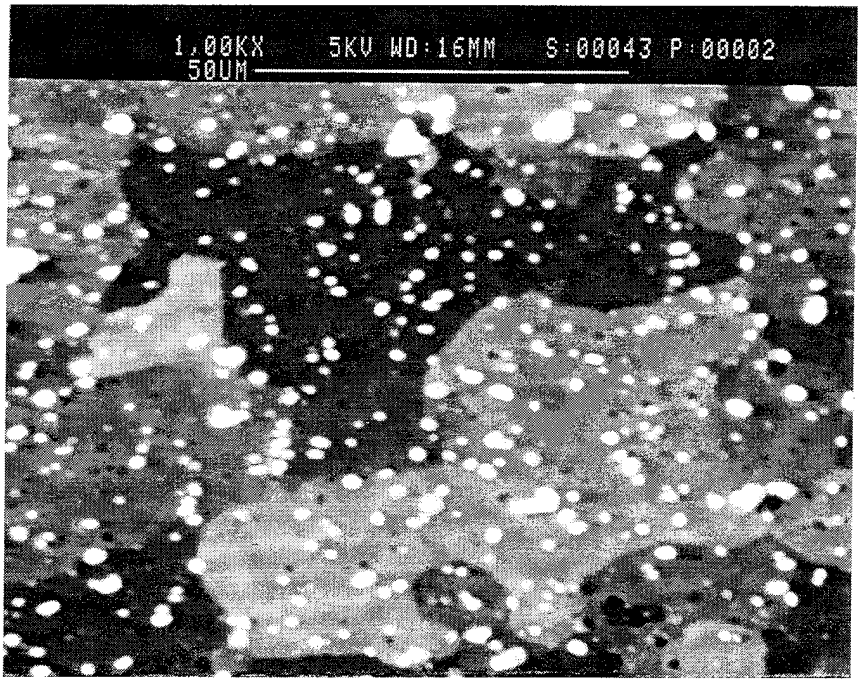

Figure 4.20 Backscattered electron micrograph of a sample overaged at 400°C for 100 hours then tested at 400°C with strain a rate of 10^{-4} sec^{-1}, grip section.

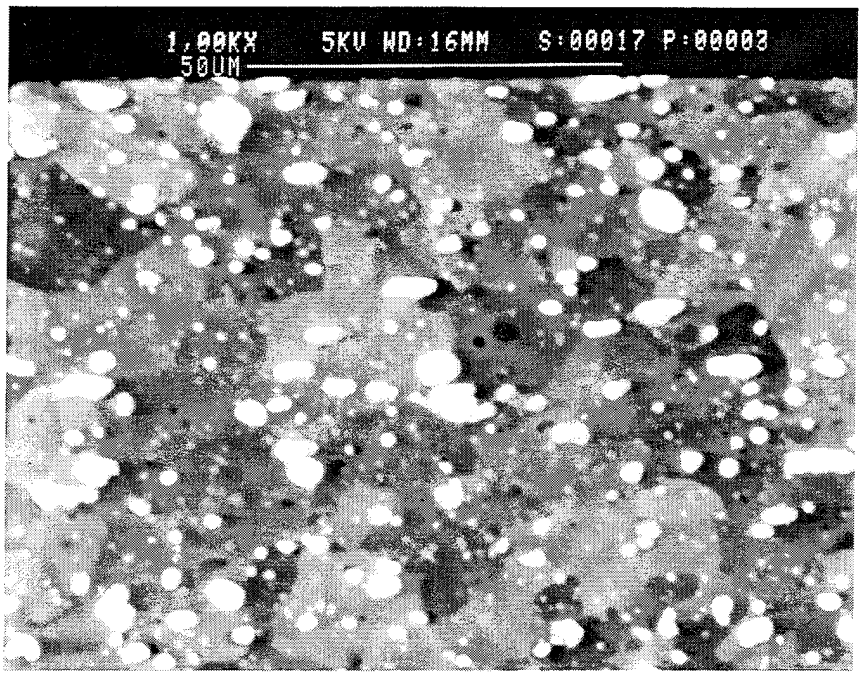

Figure 4.21 Backscattered electron micrograph of a sample overaged at 400°C for 100 hours then tested at 400°C with strain a rate of 10^{-4} sec^{-1}, grip section.

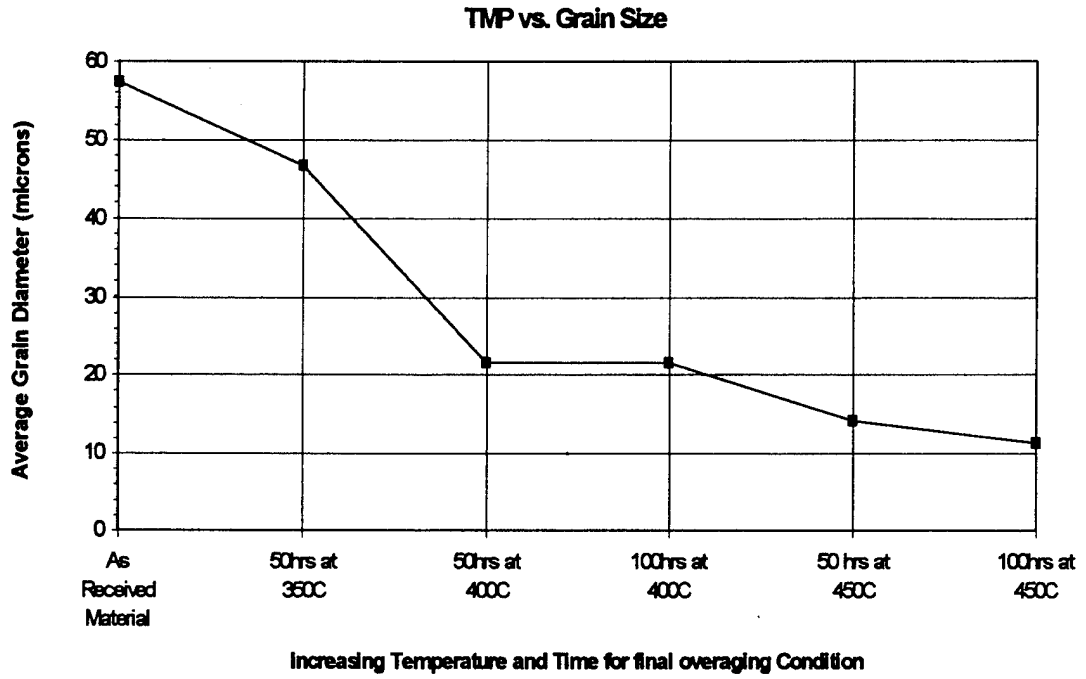

Figure 2.22 TMP versus grainsize

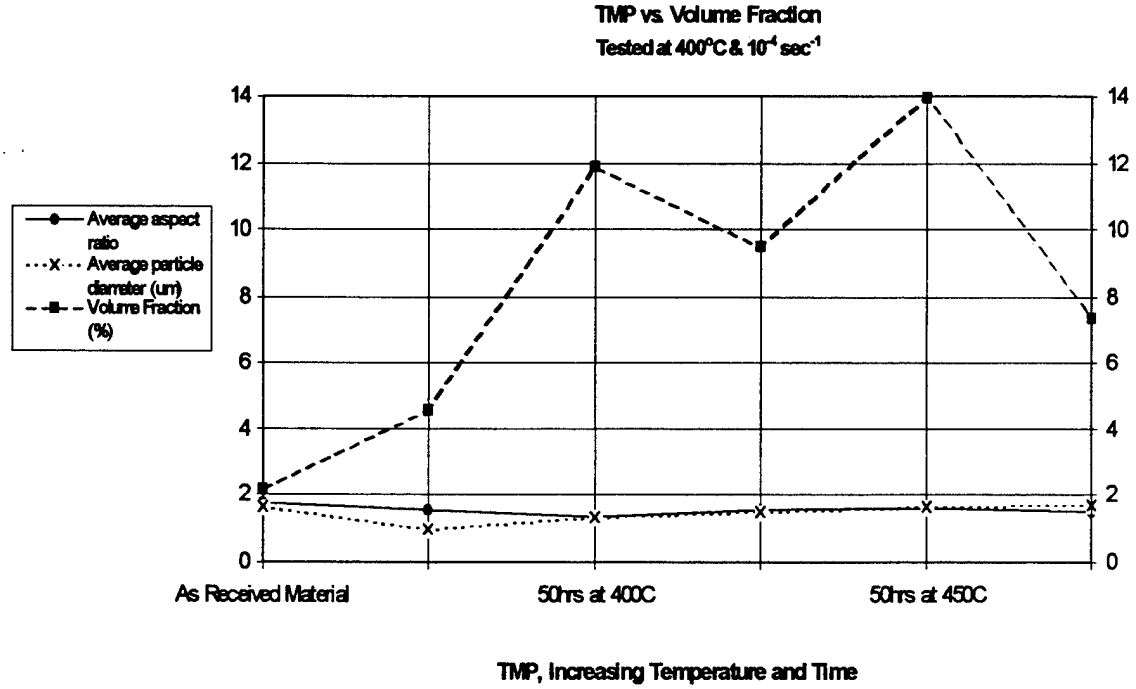

Figure 2.23 TMP versus volume fraction, particle diameter and aspect ratio

V. CONCLUSIONS AND RECOMMENDATIONS

A. CONCLUSIONS

The two major efforts of this thesis, mechanical testing and microstructural analysis, have produced enough data to form these conclusions:

1. The greatest elongation was seen in TMP25 tested at 450°C at 10^{-4} sec^{-1} strain rate. The elongation was just under 300%.

2. Most TMP's tended to result in maximum superplastic response at test temperatures equal to the prior overaging temperature.

3. Recrystallization of the aluminum matrix to the finest average diameter observed, 11.2 μm, occurred at a test temperature of 400°C for a material which had been overaged for 50 hours at 200°C then 100 hours at 450°C. The original as-received material had an average grain size of 57 microns so a reduction of almost 5 fold was achieved.

4. Specimens exhibiting the greatest superplastic elongations had equiaxed grain structures. Poor superplastic performance occurred in samples that did not fully recrystallize and hence had elongated grain structures.

5. During deformation, cavities tended to form around θ particles. Large particles were observed to have the greatest number of cavities surrounding them. This likely initiated failure in the more superplastic specimens.

B. RECOMMENDATIONS

Follow on research in this area should concentrate on the following areas:

1. TMP's at higher temperatures should be examined for this alloy, especially around 400 to 500°C. Testing of these TMP's should be at or near the overaging temperature.

2. Increased straining of the material should be done to values above 2.3. Initial thickness of the aluminum plate should be increased to the maximum allowed for the rolling mill. This would allow true strains of up to 2.8 which should reduce the final grain size, according to PSN theory.

3. Microscopy methods need to be refined in order to produce more reliable measurements of the particle size and volume fraction.

APPENDIX A: STRESS VERSUS STRAIN CURVES

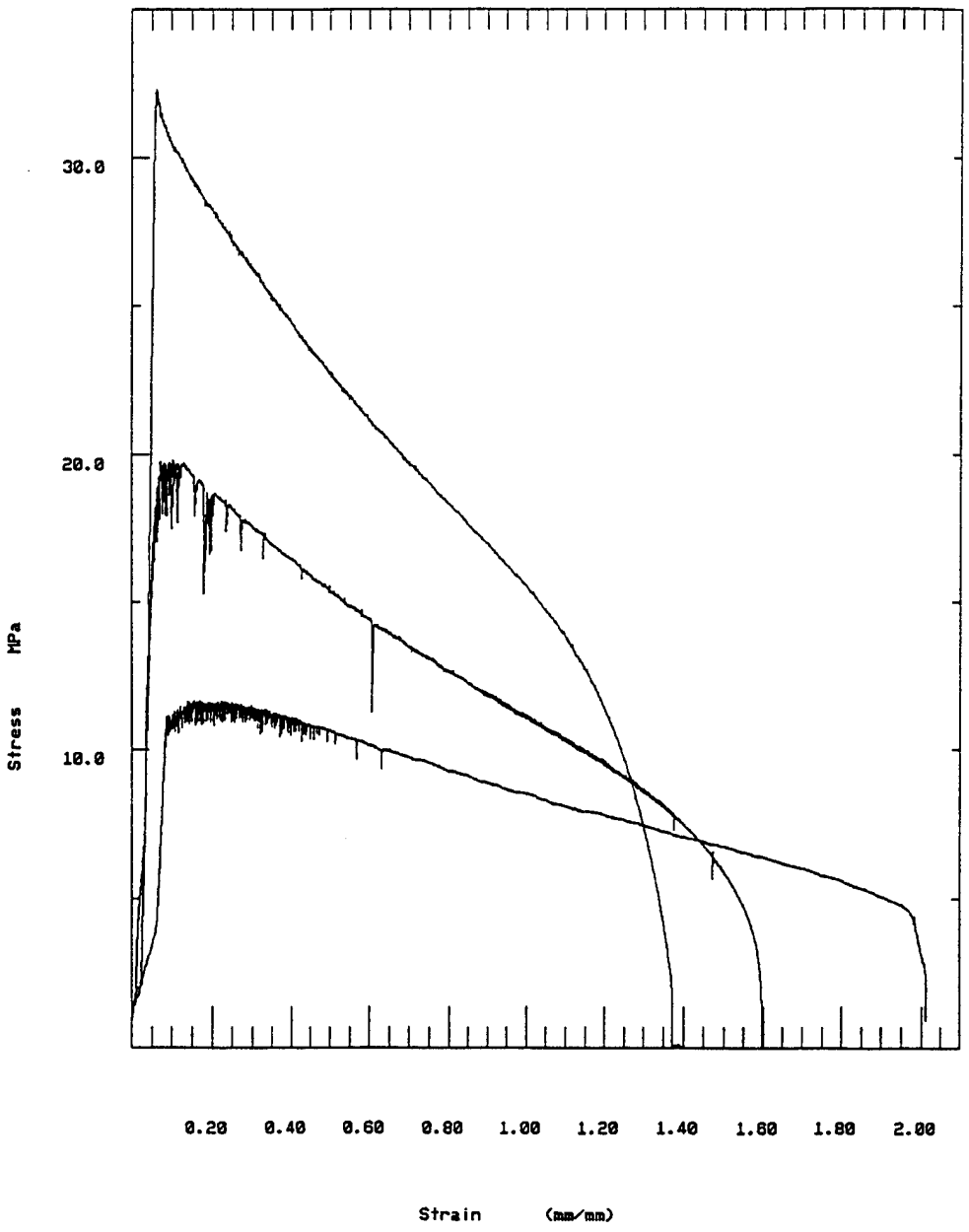

Figure A.1: Stress Versus Strain Curves for Three Tests conducted at 400°C on a material overaged at 450°C for 100 hours. Strain rates of a) 10^{-2} b) 10^{-3} c) 10^{-4} sec^{-1}.

APPENDIX B: TENSILE TEST DATA SUMMATION

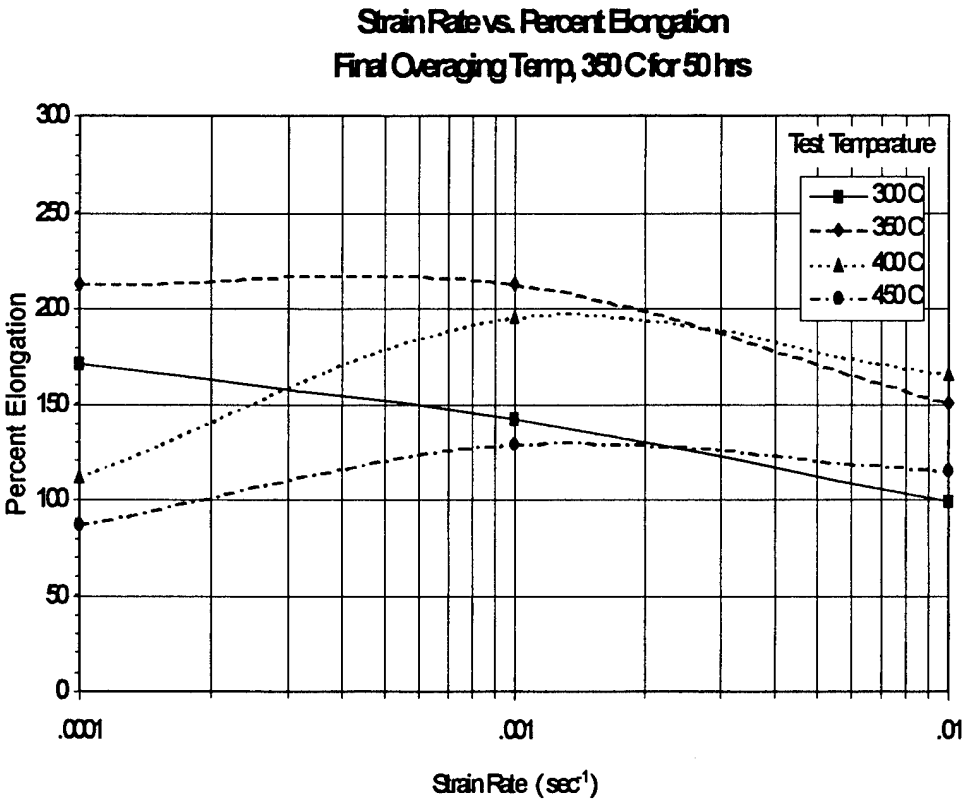

Figure B.1: Strain Rate Versus Elongation

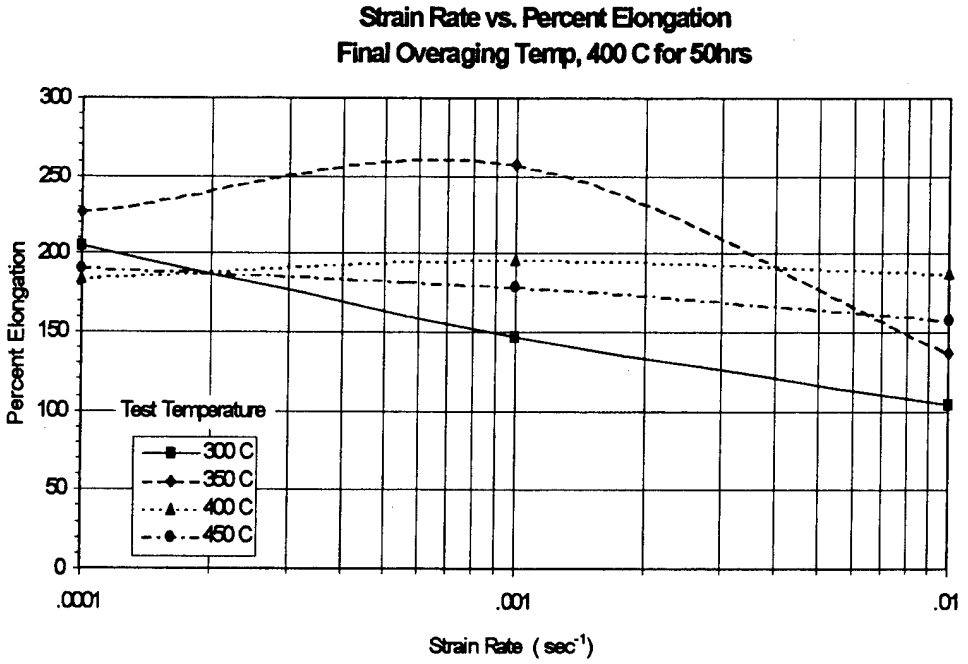

Figure B.2: Strain Rate versus Elongation

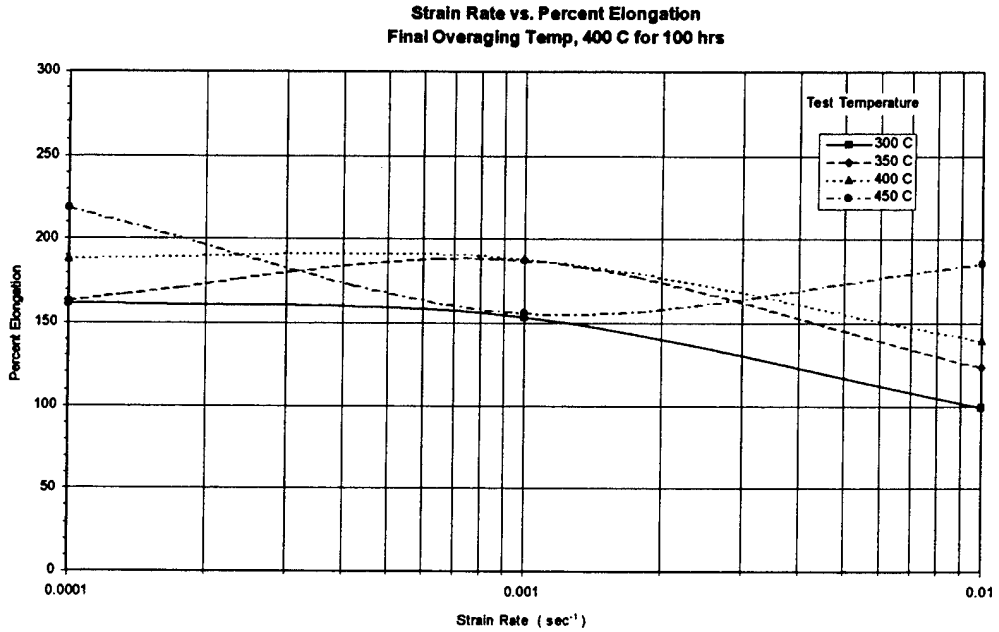

Figure B.3: Strain Rate versus Elongation

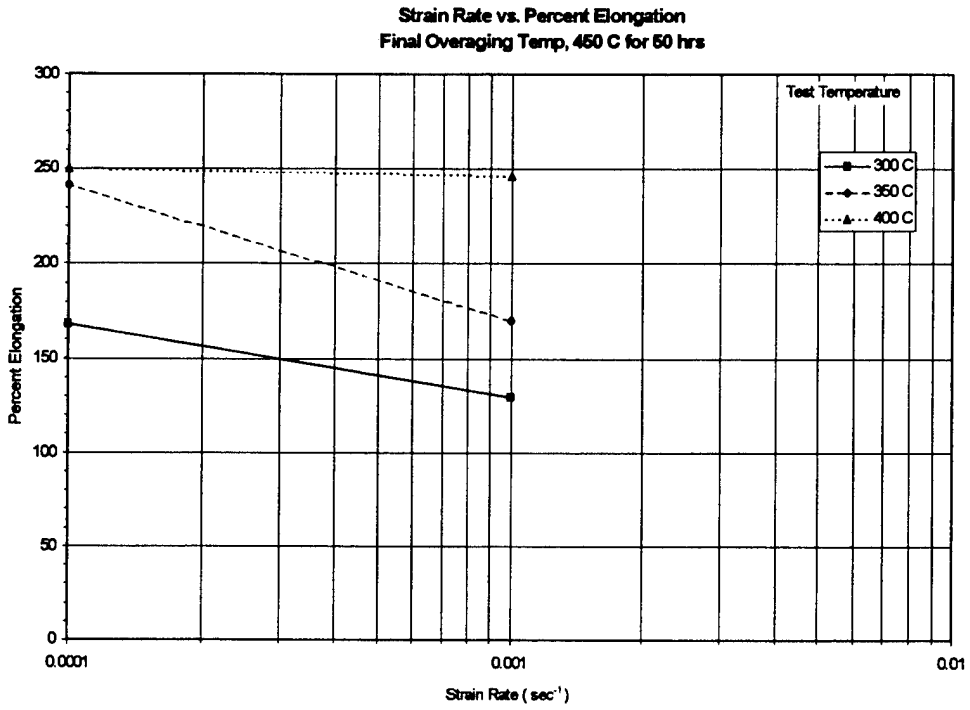

Figure B.4: Strain Rate versus Elongation

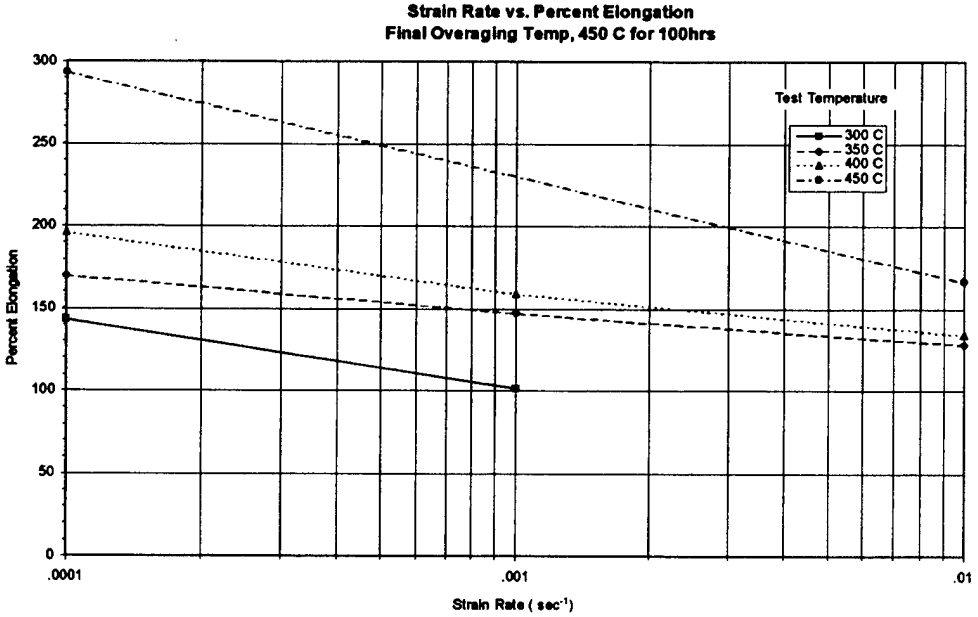

Figure B.5: Strain Rate versus Elongation

LIST OF REFERENCES

1. Wert, J.A., "Grain Refinement and Grain Size Control," *Superplastic Aluminum Alloys*, edited by Paton, N.E., and Hamilton, C.H., pp. 69-83, Conference Proceedings, TMS-AIME, Warrendale Pa., 1982.

2. Watts,B.M., Stowell, M.J., Baikie, B.L., and Owen, D.G.E., "Superplasticity in Al-CU-Zr Alloys, Part I: Material Preparation and Properties," Metal Science Journal, Vol. 10, No. 6, pp. 189-197, June 1976.

3. Baudelet, B., "Industrial Aspects of Superplasticity," *Materials Science and Engineering*, A137, pp. 41-55, 1991.

4. McNelley, T.R., and Hales, S.J., "Superplastic Aluminum Alloys," *Naval Research Reviews*, Vol. 39.1, pp.51-57, Office of Naval Research, 1987.

5. Product information, Northrop Corporation, Hawthorne, CA., Nov., 1983.

6. Northrop Corporation, Aircraft Division, Superplastic Forming: Precision Technology for Building New Generations of Aircraft, Hawthorne, CA, 1983.

7. Hales, S.J., McNelley, T.R., and McQueen, H.J., " Recrystallization and Superplasticity at 300°C in an Aluminum-Magnesium Alloy," *Metallurgical Transactions A*, Vol. 22A, pp. 1037-1047, May 1991.

8. Mathé, W., *Precipitate Coarsening During Overaging of 2519 Al-Cu alloy*: Application to Superplastic Response, Master's Thesis, Naval Postgraduate School, Monterey, CA, March 1992.

9. Bohman, S., *Thermomechanical Processing of Aluminum Alloy for Grain Refinement and Superplasticity*, Master's Thesis, Naval Postgraduate School, Monterey, CA, June 1992.

10. Dunlap, J., *Study of Refinement in Al Alloy 2519 Using Backscatter Orientation - Contrast Made in the Scanning Electron Microscope*, Master's Thesis, Naval Postgraduate School, Monterey, CA, December 1992.

11. Zohorsky, P., *Study of Precipitation and Recrystallization of Al Alloy 2519 by Backscattered Electron Imaging Methods*, Master's Thesis, Naval Postgraduate School, Monterey, CA, September 1993.

12. Callister, W. D., *Materials Science and Engineering: An Introduction*, 2nd edition, John Wiley and Sons, Inc., New York, NY, 1984.

13. Kou, S., *Welding Metallurgy*, John Wiley & Sons, New York, 1987.

14. *"Binary Alloy Phase Diagrams," American Society for Metals*, Vol. 1, Metals Park, Ohio, 1986.

15. Meyers, M. A., and Chawla, K. K., *Mechanical Metallurgy Principles and Applications*, Prentice-Hall, Inc., 1984.

16. *Metals Handbook*, 10th ed., Vol. 2, pp. 3-80, American Society for Metals, 1991.

17. Porter, D. A. and Easterling, K. E., *Phase Transformations in Metals and Alloys*, Van Nostrand Reinhold Co., Ltd., Workingham, England, 1988.

18. Pilling, J., and Ridley, N., *Superplasticity in Crystalline Solids*, The Institute of Metals, 1989.

19. Crooks, R., Hales, S.J., and McNelley, T.R., "Microstructural Refinement via Continuous Recrystallization in a Superplastic Aluminum Alloy," *Superplasticity and Superplastic Forming*, edited by Hamilton, C.H. and Paton, N.E., pp. 389-393, The Minerals, Metals, & Materials Society, 1988.

20. Hamilton, C. H., Bampton, C. C., and Paton, N. E., "Superplasticity in High Strength Aluminum Alloys," *Superplastic Forming of Structural Alloys*, ed. N. E. Paton and C.H. Hamilton, Conference proceedings, TMS-AIME, Warrendale, PA, pp. 173-189, 1982.

21. Humphreys, F. J., "Local Lattice Rotations at Second Phase Particles in Deformed Metals," *Acta Metallurgica*, Vol. 27, pp. 1801-1814, 1979.

22. Ashby, M. F., *Philos. Metall.*, 21 (1970) 399.

23. Argon, A. S., Im, J. and Safoglu, R., "Cavity Formation From Inclusions in Ductile Fracture," *Metallurgical Transactions*, Vol. 6A, p.82, 1975.

24. Humphreys, F. J., Acta. Metall., 25 (1977) 1323.

25. McNelley, T. R., Crooks, R., Kalu, P. N., Rogers, S.A., "Precipitation and Recrystallization During Processing of a Superplastic Al-10Mg-0.1Zr Alloy," *Material Science and Engineering*, A166, pp. 135-143, 1993.

26. Willig, V., and Heimendahl, M., "*Problems of Particle Coarsening of Disk Shaped Particles in Aluminum Alloy 2219*," Institut fur Wefkstoffwissenschaften 1 der Universitas Erlangen, Nurnberg, 647-681, 1979.

INITIAL DISTRIBUTION LIST

1.	Defense Technical Information Center Cameron Station Alexandria, VA 22304-6145	2
2.	Library, Code 52 Naval Postgraduate School Monterey, CA 93943-5002	2
3.	Naval Engineering, Code 34 Naval Postgraduate School Monterey, CA 93943-5100	1
4.	Department Chairman, Code ME/Kk Department of Mechanical Engineering Naval Postgraduate School Monterey, CA 93943-5000	1
5.	Professor T. R. McNelley, Code ME/Mc Department of Mechanical Engineering Naval Postgraduate School Monterey, CA 93943-5000	4
6.	Benjamin B. Peet 8345 Torrell Way San Diego, CA 92126	2